

Band structure calculations for strongly correlated materials using LDA+DMFT

Nils Blümer, Univ. Mainz

Outline

Band structures and effects of strong electronic correlations

Approaches for correlated electron systems \rightsquigarrow DMFT

The LDA+DMFT method: setup and applications

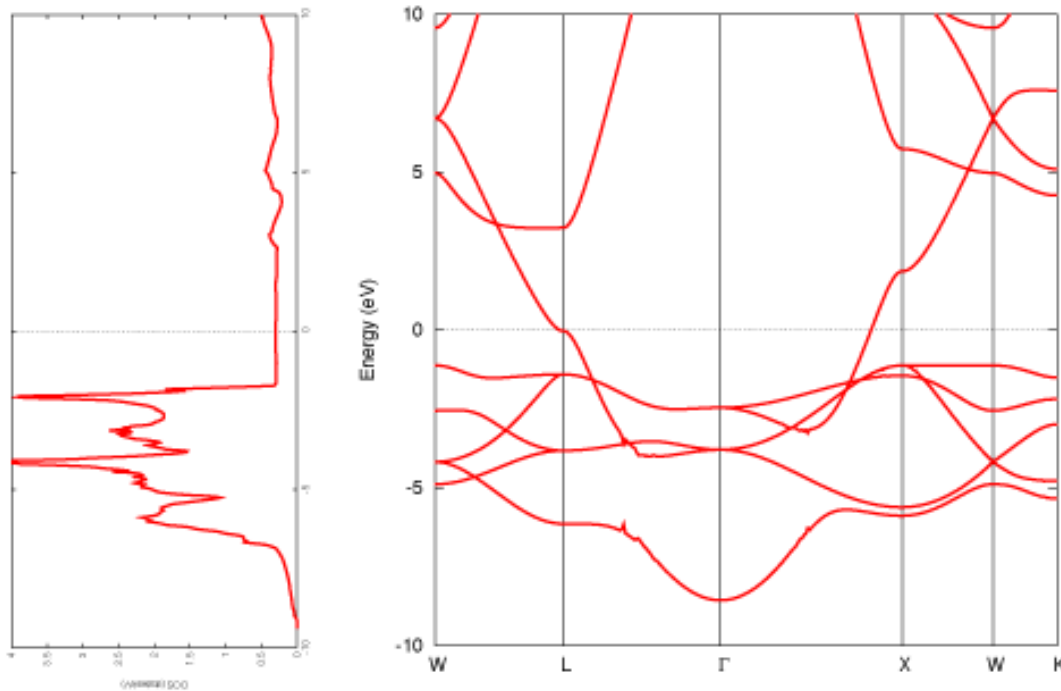
Auxiliary-field quantum Monte Carlo algorithm

QMC DMFT solvers: recent developments

Summary and outlook

Motivation: band structures and effects of strong electronic correlations

Conventional band structure results (here for fcc Au)



Density functional theory (DFT)
 \rightsquigarrow bands with dispersion $\varepsilon_{n,\mathbf{k}}$
 \mathbf{k} integration \rightsquigarrow spectra $A(\varepsilon)$

How? Use \mathbf{k} -resolved spectral function $A(\mathbf{k}, \varepsilon) = \sum_n \delta(\varepsilon - \varepsilon_{n,\mathbf{k}})$

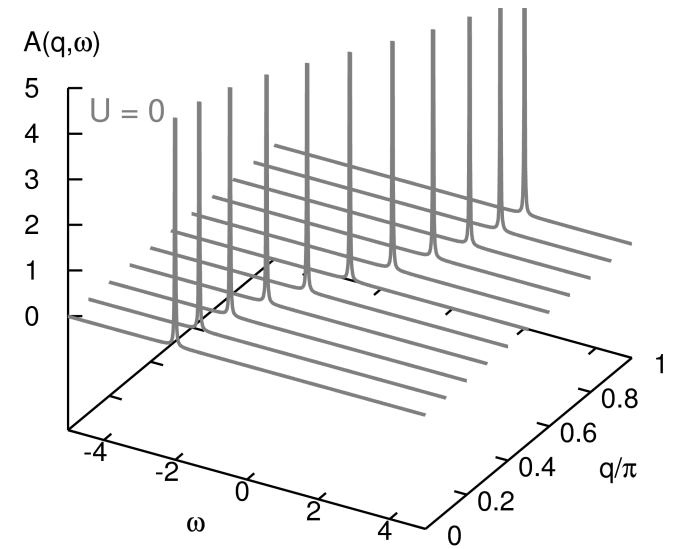
$$\rightsquigarrow A(\varepsilon) = \frac{1}{V_B} \int d^3k A(\mathbf{k}, \varepsilon)$$

Note: all contributions to $A(\mathbf{k}, \varepsilon)$ are singular!

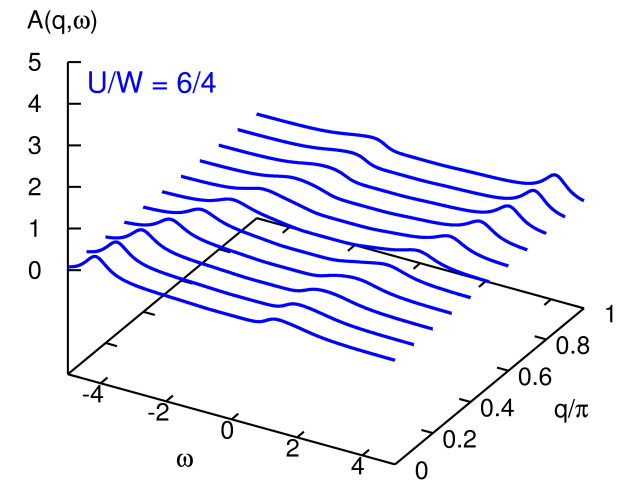
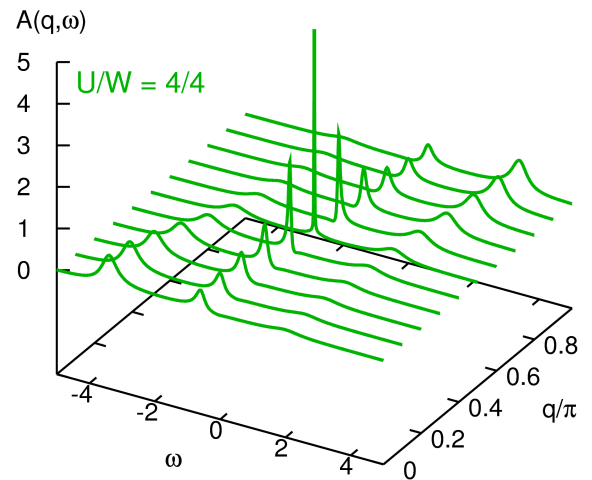
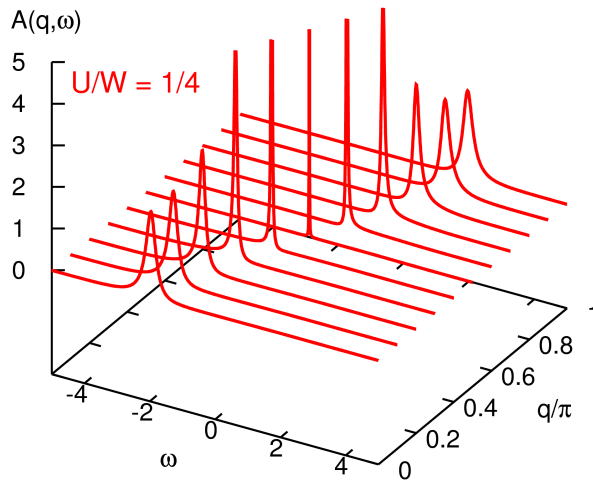
Is this physical? No: correlations lead to finite lifetimes \sim broadening of $A(\mathbf{k}, \varepsilon)$!

Illustration: single-band model

(i) tight-binding model of independent electrons
($q \sim k_x, \omega \sim \varepsilon$)



(ii) Hubbard model with local electron-electron interaction U (at half filling)



Better italian cuisine: lasagne, not spaghetti!

Goals of LDA+DMFT

Capture strong-correlation effects, e.g., Mott transition: **beyond** ○ LDA ○ DFT?

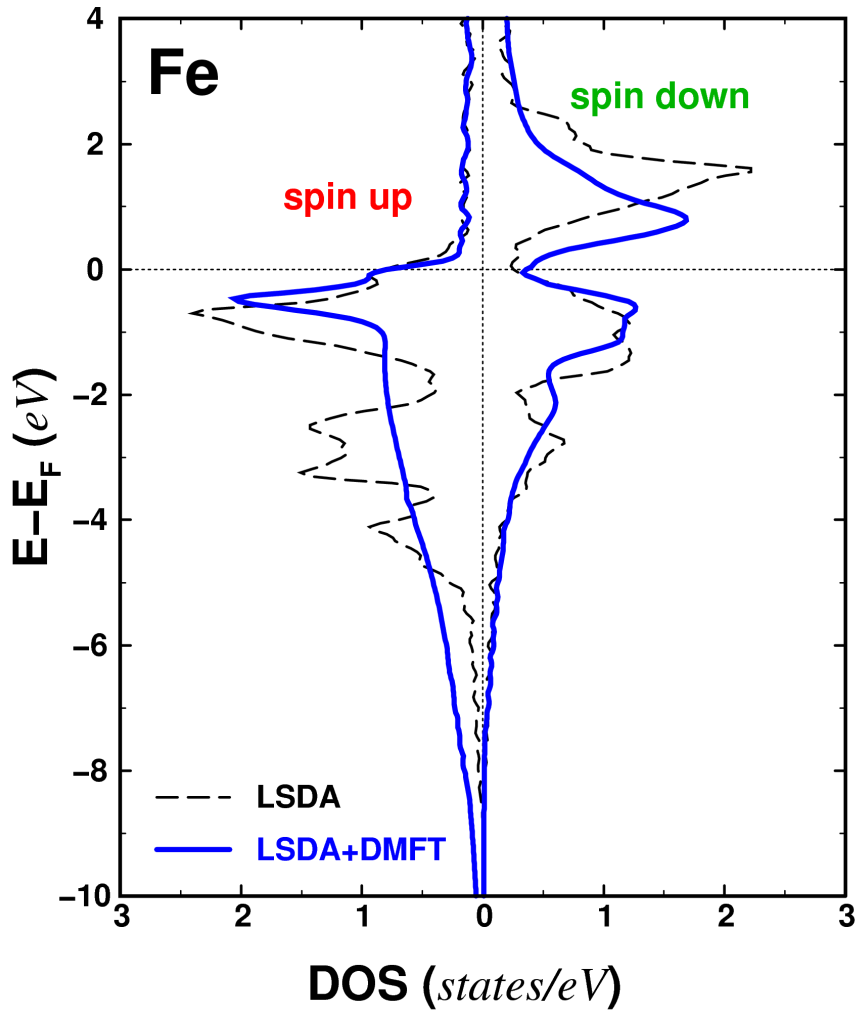
But also weak-correlation effects:

beyond DFT: “spaghetti” $\xrightarrow{\Sigma(\omega)}$ “lasagne”

beyond DFT: calculate transition temperatures, e.g., Curie temperature

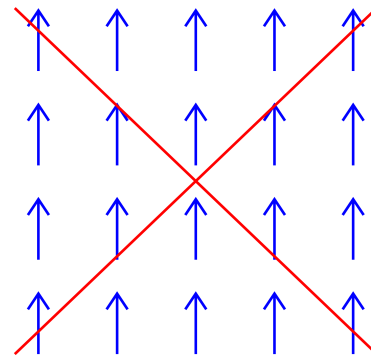
beyond LDA: correct gaps, moments, equilibrium volume. . .

Effects of strong correlations: Itinerant ferromagnetism and half-metallicity



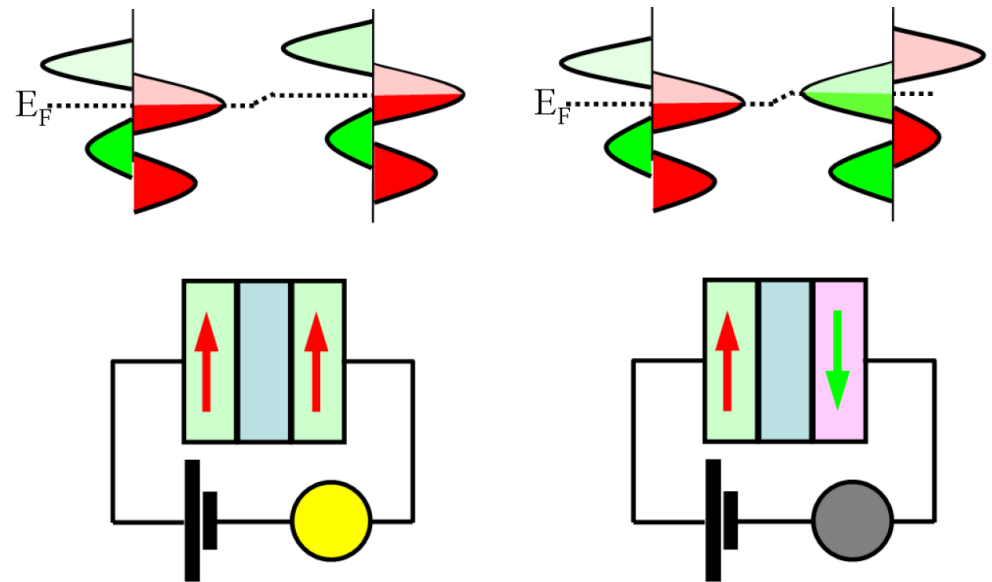
[Chioncel et. al, PRB (2003)]

Qualitatively captured by LDA, modifications in LDA+DMFT



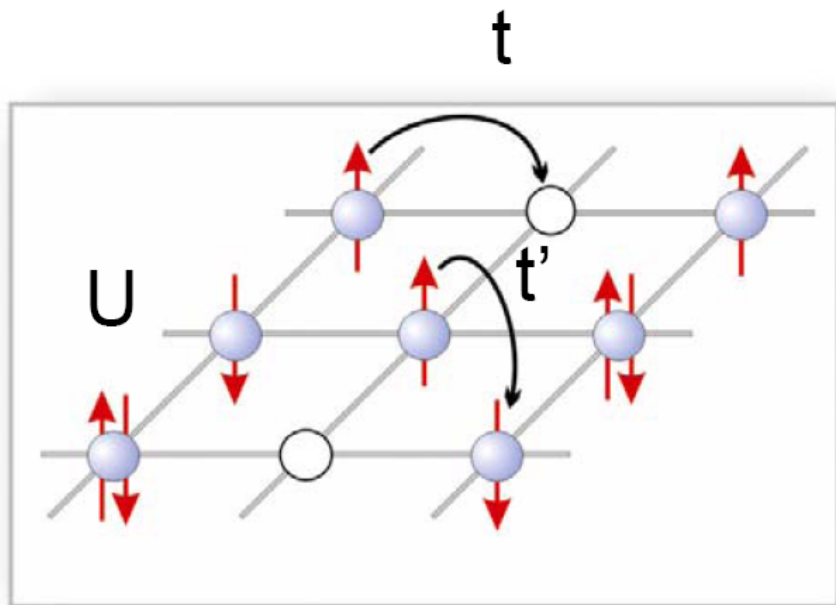
Spin models
insufficient

Technological goal: TMR with half metals

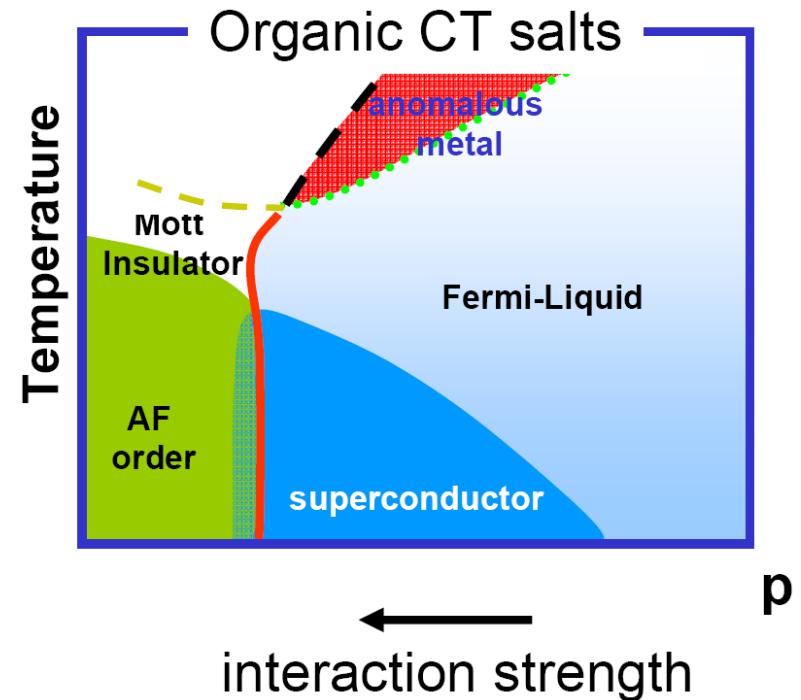
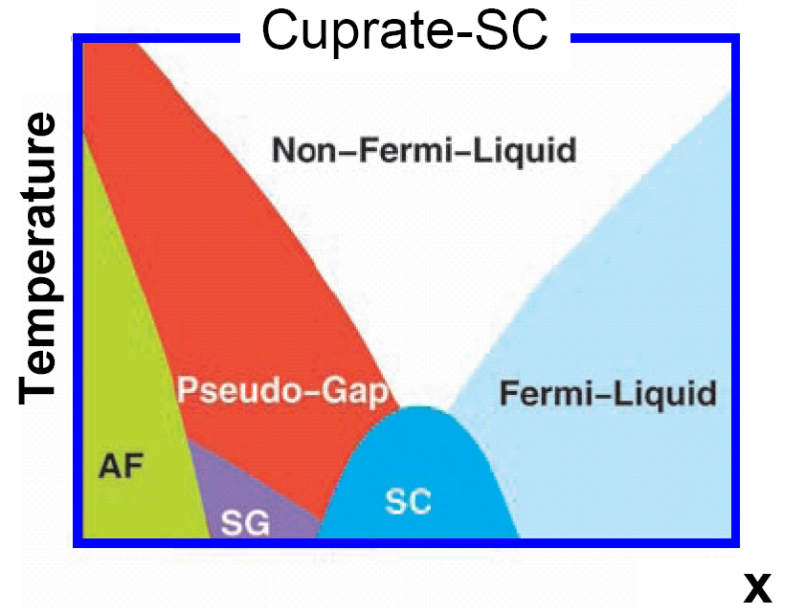


Complex phases of cuprate and organic superconductors

High- T_c physics contained in 2D Hubbard model?



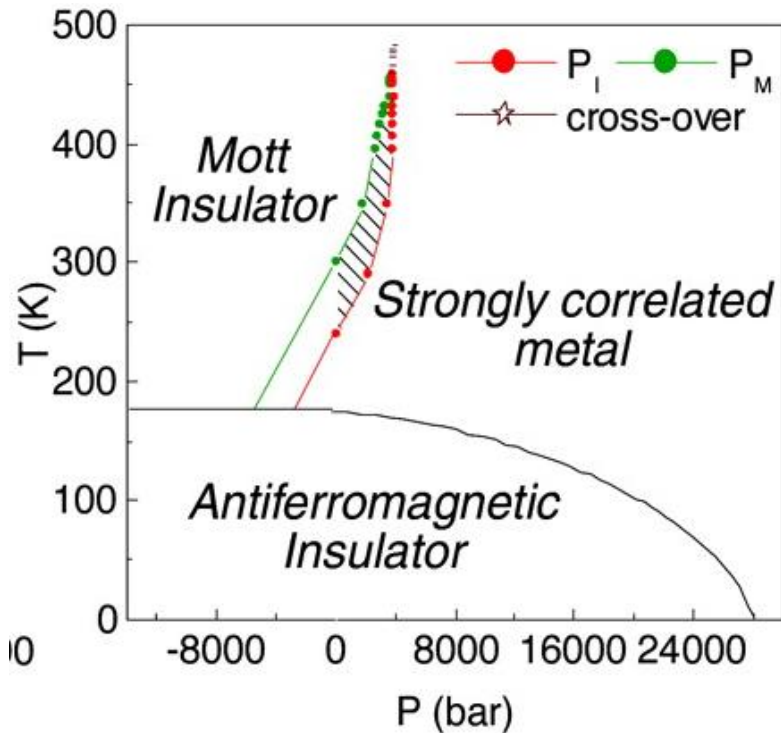
Are antiferromagnetic (AF) and Mott insulating phases essential for superconductivity?



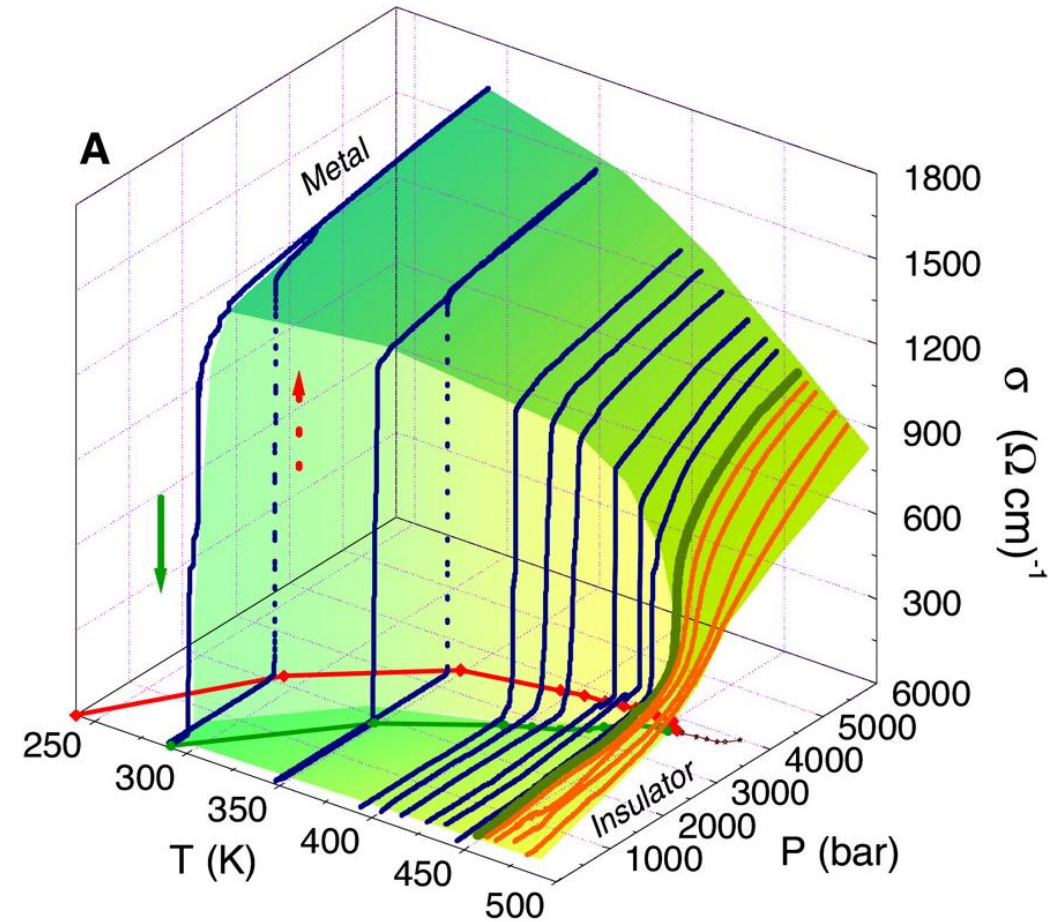
Mott metal-insulator transition

Prototype example: V_2O_3 doped with Cr/Ti and/or under pressure

Phase diagram



Electrical conductivity



[Limelette et al., Science 302, 89 (2003)]

No paramagnetic Mott insulator (spin degeneracy, no doubling of unit cell) in DFT!

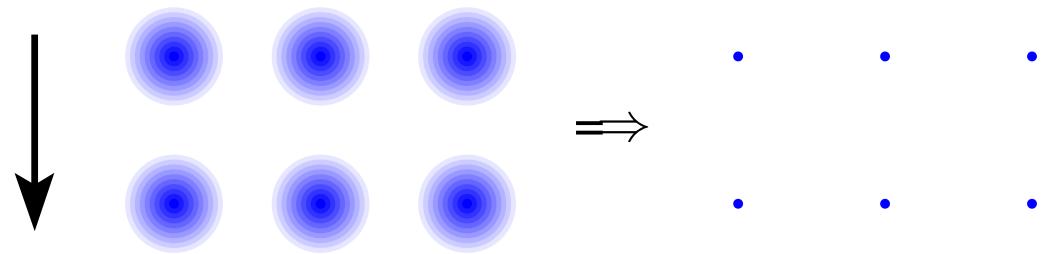
Approaches for correlated electron systems

Microscopic modeling I

General Hamiltonian for nuclei and electrons

$$H = \sum_{i=1}^{N_e} \frac{\mathbf{p}_i^2}{2m} + \sum_{k=1}^L \frac{\mathbf{P}_k^2}{2M_k} + \sum_{k<l} \frac{Z_k Z_l e^2}{|\mathbf{R}_k - \mathbf{R}_l|} - \sum_{i,k} \frac{Z_k e^2}{|\mathbf{r}_i - \mathbf{R}_k|} + \sum_{i<j} \frac{e^2}{|\mathbf{r}_i - \mathbf{r}_j|}$$

Born-Oppenheimer approximation (0th order)



$$H = \sum_{i=1}^{N_e} \frac{\mathbf{p}_i^2}{2m} + \sum_i V(\mathbf{r}_i) + \sum_{i<j} \frac{e^2}{|\mathbf{r}_i - \mathbf{r}_j|}$$

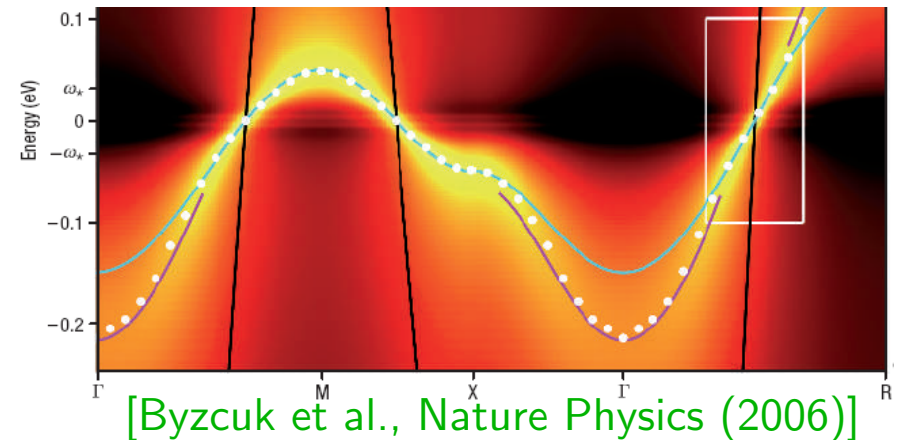
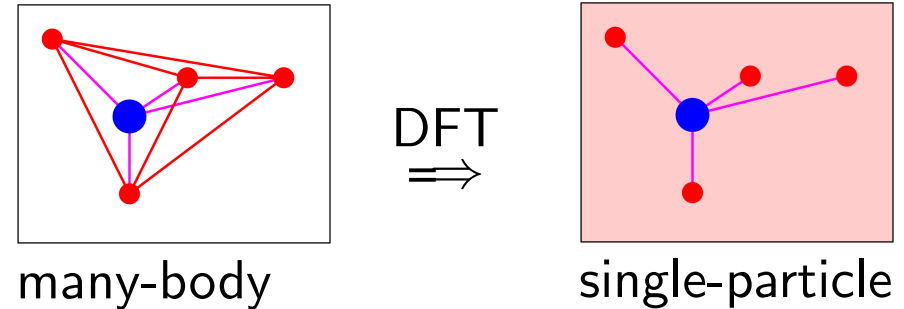
Classes of theoretical approaches for electronic problem

- continuum methods: density functional theory (DFT), variational+diffusion QMC, . . .
- methods for lattice electrons

Density functional theory in LDA

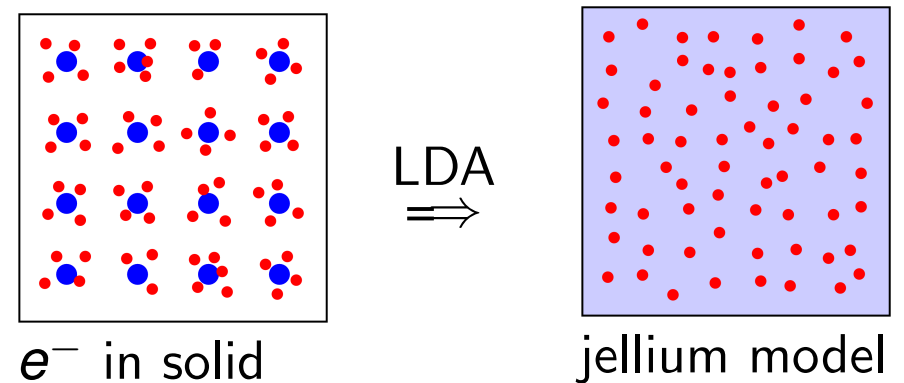
Density functional theory (DFT)

- exact ground state approach
- based on electron density $\rho(\mathbf{r})$
- Kohn-Sham equations solve effective single-particle problem
- result: ground state energy + $\rho(\mathbf{r})$
- heuristics: band structure
- problem: exchange-correlation potential unknown



Local density approximation (LDA)

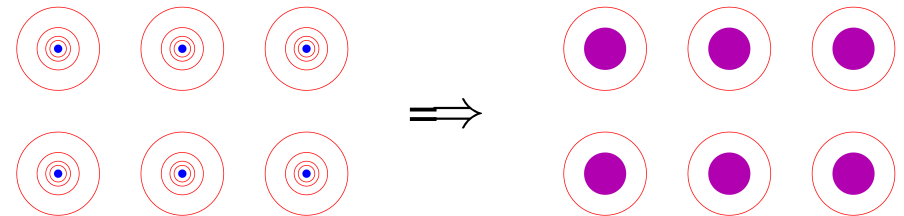
- exchange-correlation potential from jellium model (parametrized QMC)
- not reliable for correlated systems
- often good results
- basis for LDA+U and LDA+DMFT



Microscopic modeling II

$$H = \sum_{i=1}^{N_e} \frac{\mathbf{p}_i^2}{2m} + \sum_i V(\mathbf{r}_i) + \sum_{i < j} \frac{e^2}{|\mathbf{r}_i - \mathbf{r}_j|}$$

reduction to valence electrons



$$H = \sum_{i=1}^{N_v} \frac{\mathbf{p}_i^2}{2m} + \sum_{i=1}^{N_v} V^{\text{ion}}(\mathbf{r}_i) + \sum_{i=1}^{N_v-1} \sum_{j=i+1}^{N_v} V^{ee}(\mathbf{r}_i, \mathbf{r}_j)$$

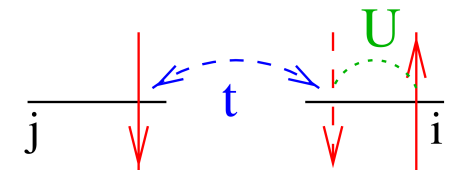
occupation number formalism

Wannier orbitals

$$\hat{H} = \sum_{i\nu j\sigma} t_{ij}^{\nu} \hat{c}_{i\nu\sigma}^{\dagger} \hat{c}_{j\nu\sigma} + \frac{1}{2} \sum_{\nu\nu'\mu\mu'} \sum_{ijmn} \sum_{\sigma\sigma'} \mathcal{V}_{ijmn}^{\nu\nu'\mu\mu'} \hat{c}_{i\nu\sigma}^{\dagger} \hat{c}_{j\nu'\sigma'}^{\dagger} \hat{c}_{n\mu'\sigma'} \hat{c}_{m\mu\sigma}$$

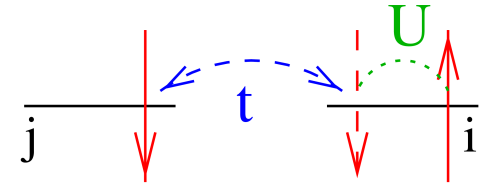
Hubbard model

$$\hat{H} = \sum_{(i,j),\sigma} t_{ij} (\hat{c}_{i\sigma}^{\dagger} \hat{c}_{j\sigma} + \text{h.c.}) + U \sum_i \hat{n}_{i\uparrow} \hat{n}_{i\downarrow}$$



Approaches for Hubbard-type models

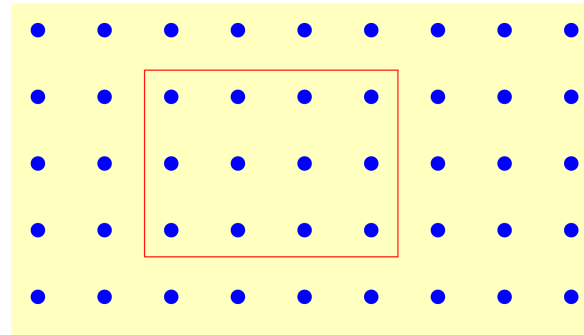
$$\hat{H} = \sum_{(i,j),\sigma} t_{ij} (\hat{c}_{i\sigma}^\dagger \hat{c}_{j\sigma} + \text{h.c.}) + U \sum_i \hat{n}_{i\uparrow} \hat{n}_{i\downarrow}$$



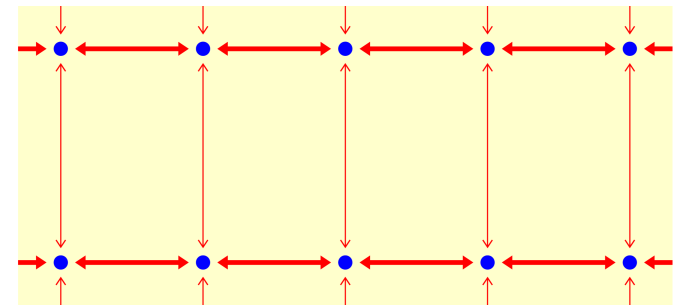
Perturbation theory

- $U \rightarrow 0$: Hartree-Fock
2nd order PT, . . .
- $t/U \rightarrow 0$ (for $n = 1$)
 \rightsquigarrow Heisenberg model

finite clusters: ED, QMC



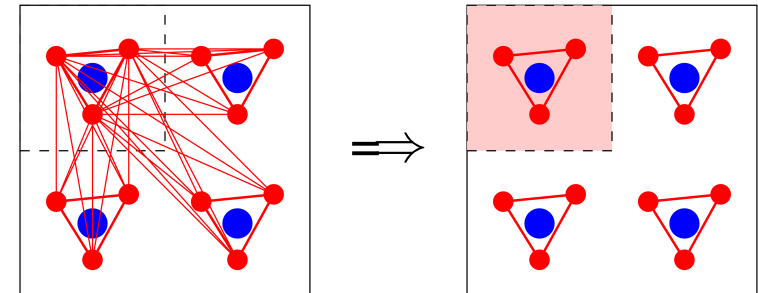
$d \rightarrow 1$: Bethe ansatz, DMRG



Dynamical mean-field theory (DMFT): local self-energy $\Sigma(\mathbf{k}, \omega) \equiv \Sigma(\omega)$

[Metzner, Vollhardt, PRL (1989), Georges, Kotliar, PRL (1992), Jarrell, PRL (1992)]

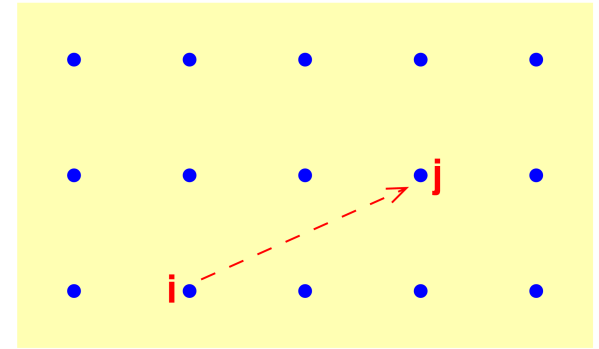
- + non-perturbative \rightsquigarrow valid at MIT
- + dynamical on-site correlations preserved
- + in thermodynamic limit
- +/- exact for coordination $Z \rightarrow \infty$



Excursus: Green function and self-energy

Single-particle Green function (lattice sites i, j):

$$G_{ij}(t_1, t_2) = -\langle c_j(t_2) c_i^\dagger(t_1) \rangle$$

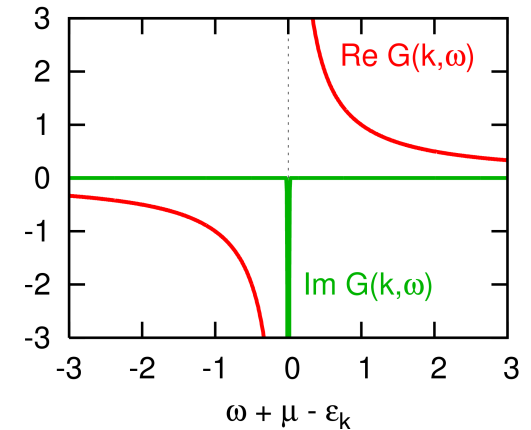


Translation invariance in space and time: $G_{ij}(t_1, t_2) \equiv G_{j-i}(t_2 - t_1) \xrightarrow{\text{Fourier}} G(\mathbf{k}, \omega)$

Noninteracting limit (dispersion $\varepsilon_{\mathbf{k}}$): $G^0(\mathbf{k}, \omega) = \frac{1}{\omega + \mu - \varepsilon_{\mathbf{k}}}$

Self-energy Σ quantifies impact of interactions:

$$G(\mathbf{k}, \omega) = \frac{1}{\omega + \mu - \varepsilon_{\mathbf{k}} - \Sigma(\mathbf{k}, \omega)}$$



Locality of self-energy $\Sigma(\mathbf{k}, \omega) \equiv \Sigma(\omega)$ within DMFT simplifies local Green function:

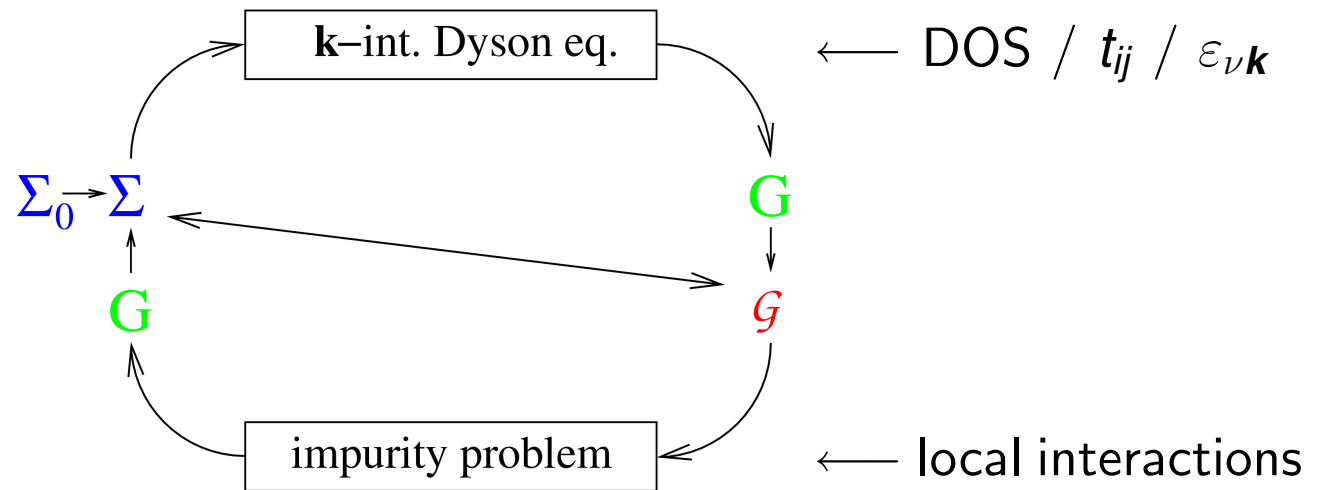
$$G(\omega) \equiv G_{ij}(\omega) = \int d\varepsilon \frac{N^0(\varepsilon)}{\omega + \mu - \varepsilon - \Sigma(\omega)}; \quad N^0(\varepsilon) = \frac{1}{N} \sum_{\mathbf{k}} \delta(\varepsilon - \varepsilon_{\mathbf{k}})$$

k integrated Dyson equation

noninteracting DOS

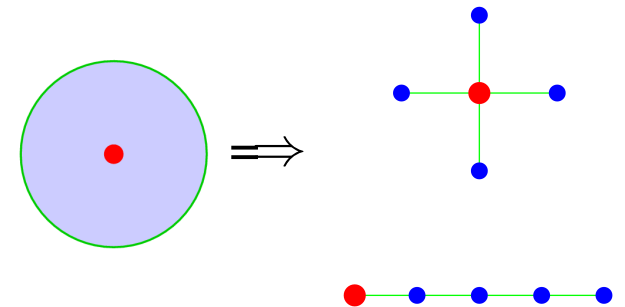
Iterative solution of DMFT equations

0. Initialize self-energy
1. Solve Dyson equation
2. Solve **single impurity Anderson model (SIAM)**



Impurity solver:

- Iterative perturbation theory (IPT; not controlled)
- Quantum Monte-Carlo (QMC)
- Exact diagonalization (ED; large finite-size errors)
- Numerical renormalization group (NRG; 1-2 bands)
- Density matrix renormalization group (DMRG)
- Self-energy functional theory (SFT) + ED



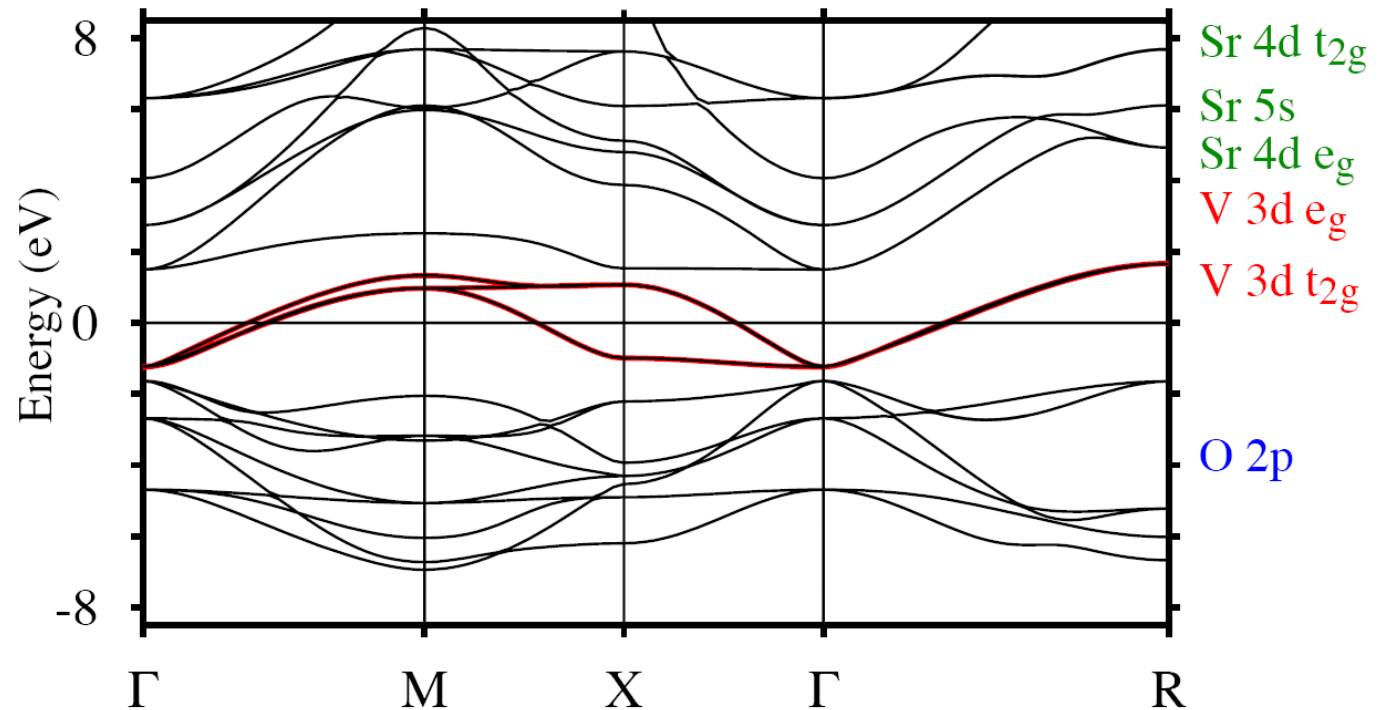
LDA+DMFT method: setup and applications

LDA+DMFT philosophy:

Interactions among extended orbitals well screened; should be captured by LDA.

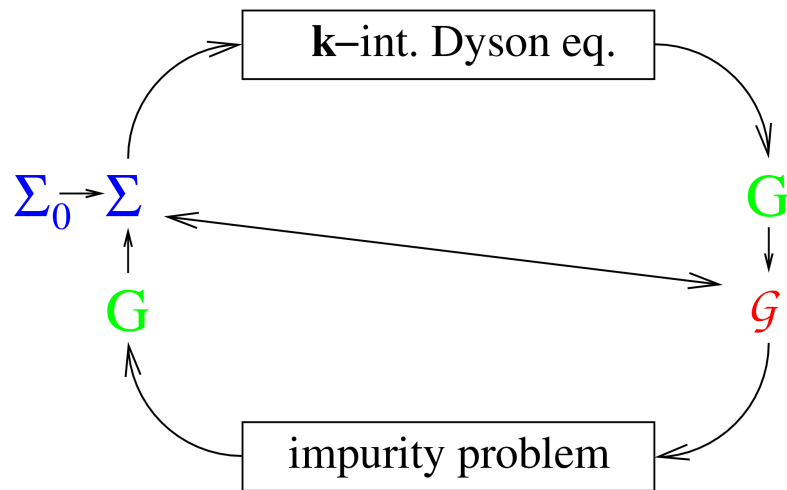
Many-body treatment (only) for narrow bands near Fermi energy (typically 3d, 4f)

Example: SrVO₃
(cubic perovskite) –
NMTO bands with
downfolding to V 3d
*t*_{2g} bands

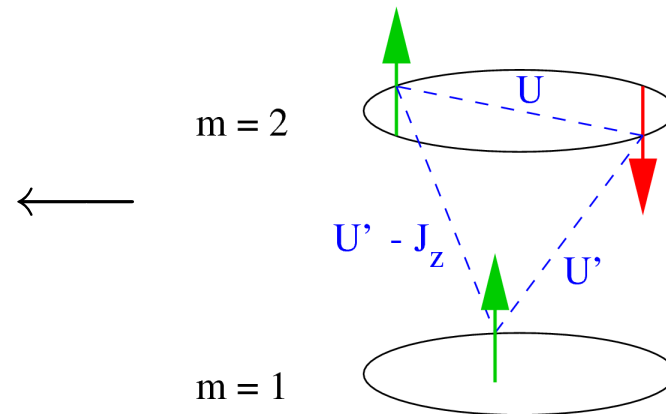


Here: simplest case – all correlated bands are equivalent

LDA+DMFT for M equivalent bands ($m = 1 \dots M$)



$$G^{m,\sigma}(\omega) \equiv G_{ii}^{m,\sigma}(\omega) = \int d\varepsilon \frac{N^{\text{LDA}}(\varepsilon)}{\omega + \mu - \varepsilon - \Sigma(\omega)}$$



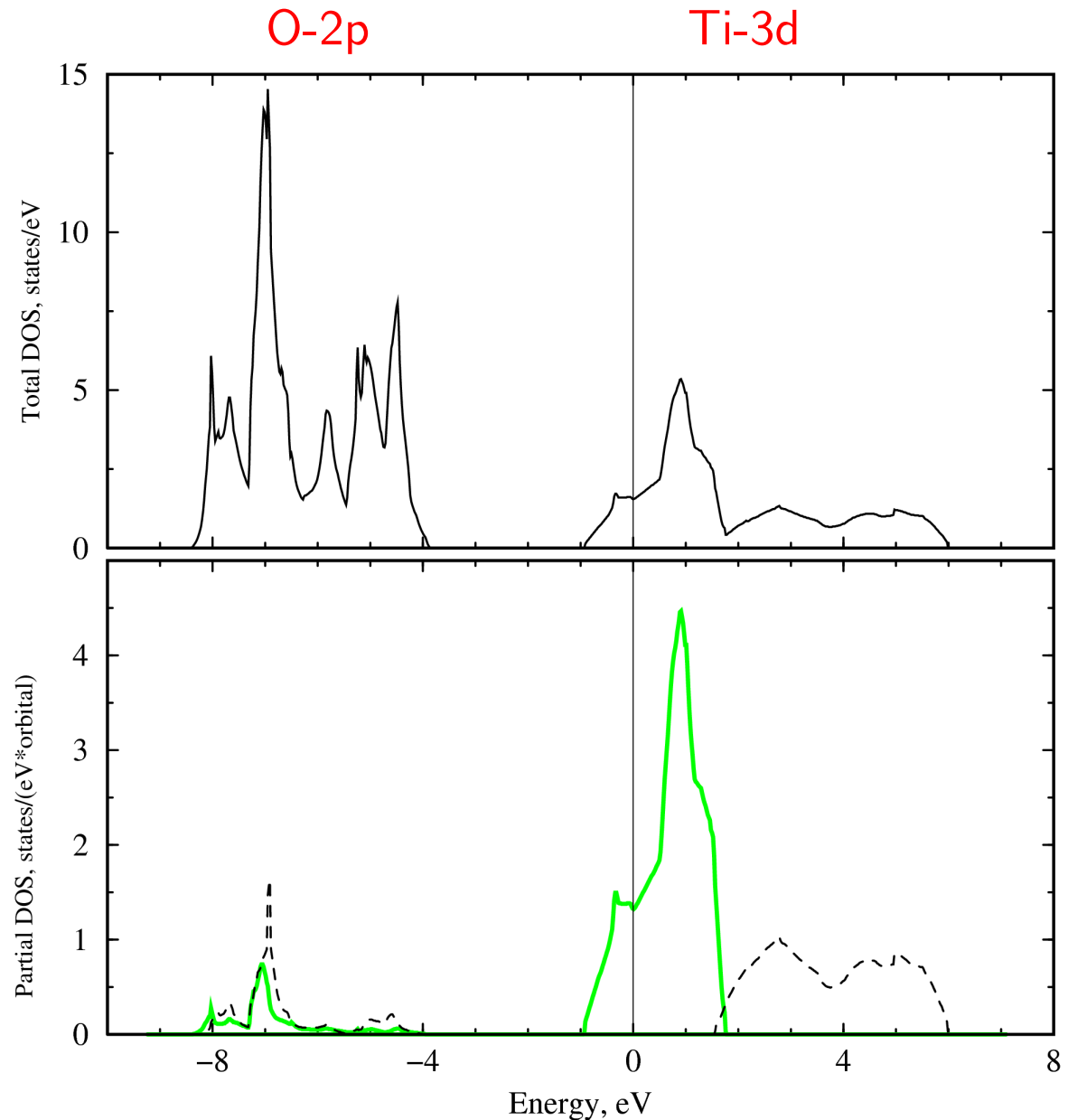
Interaction parameters U , U' , J : e.g. from [constrained LDA](#)

Early example:

perovskite $\text{La}_{1-x}\text{Sr}_x\text{TiO}_3$
($x = 0.06$)

TB-LMTO-ASA calculation
(for $x = 0$, cubic unit cell)

Spectral weight near Fermi energy:
nearly pure $3d t_{2g}$ character



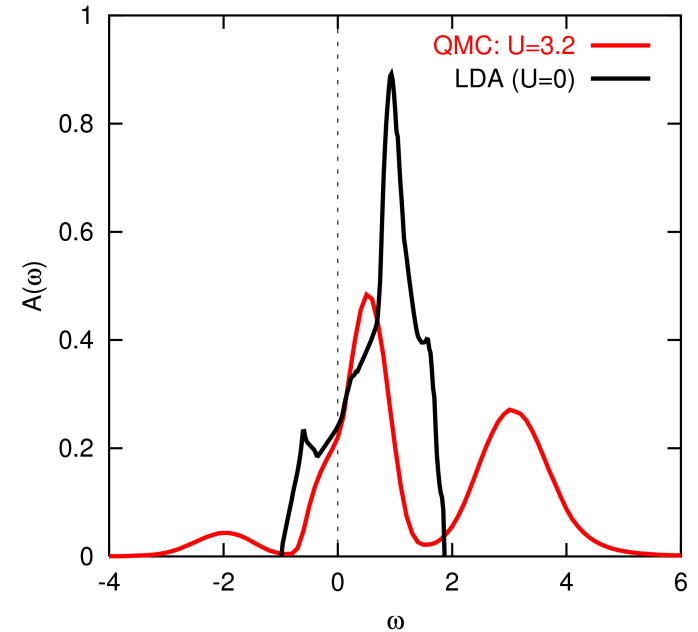
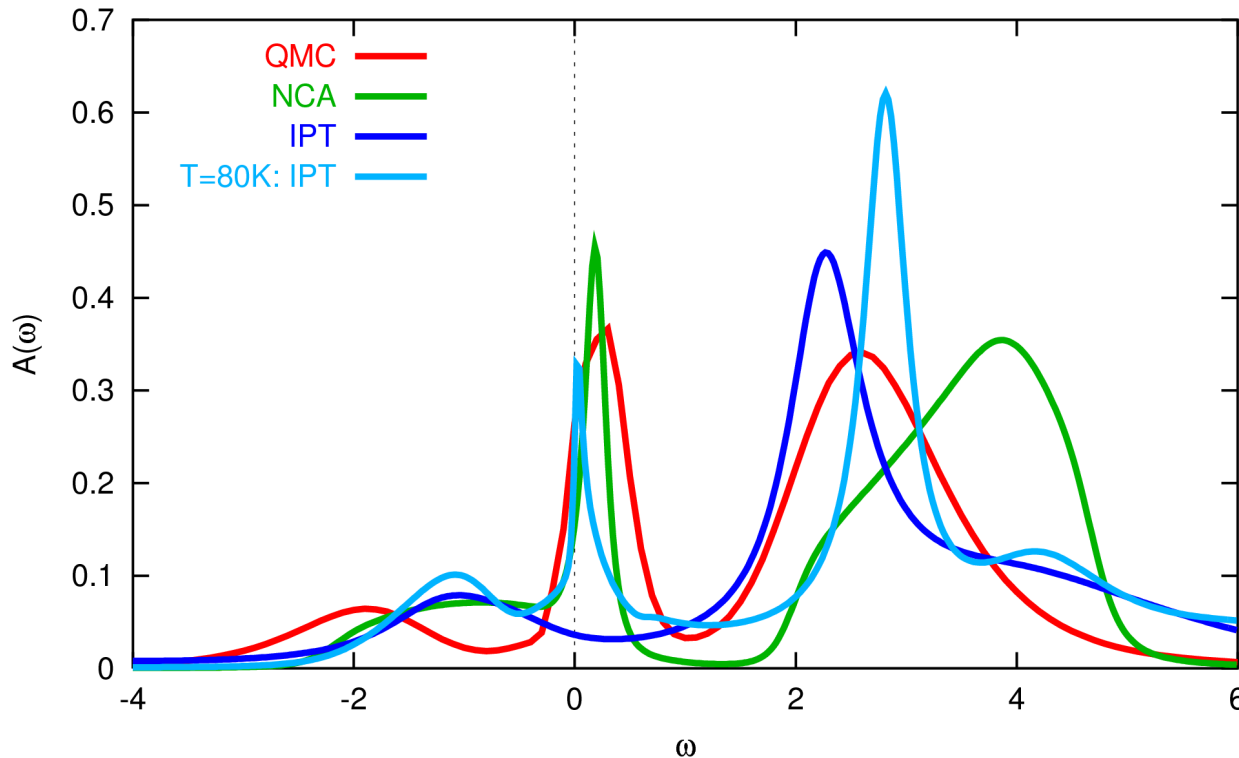
[I.A. Nekrasov, K. Held, NB, A.I. Poteryaev, V.I. Anisimov, and D. Vollhardt, EPJP 18, 55 (2000)]

Impact of correlations?

$$U = U' = 3.2 \text{ eV}, J = 0$$

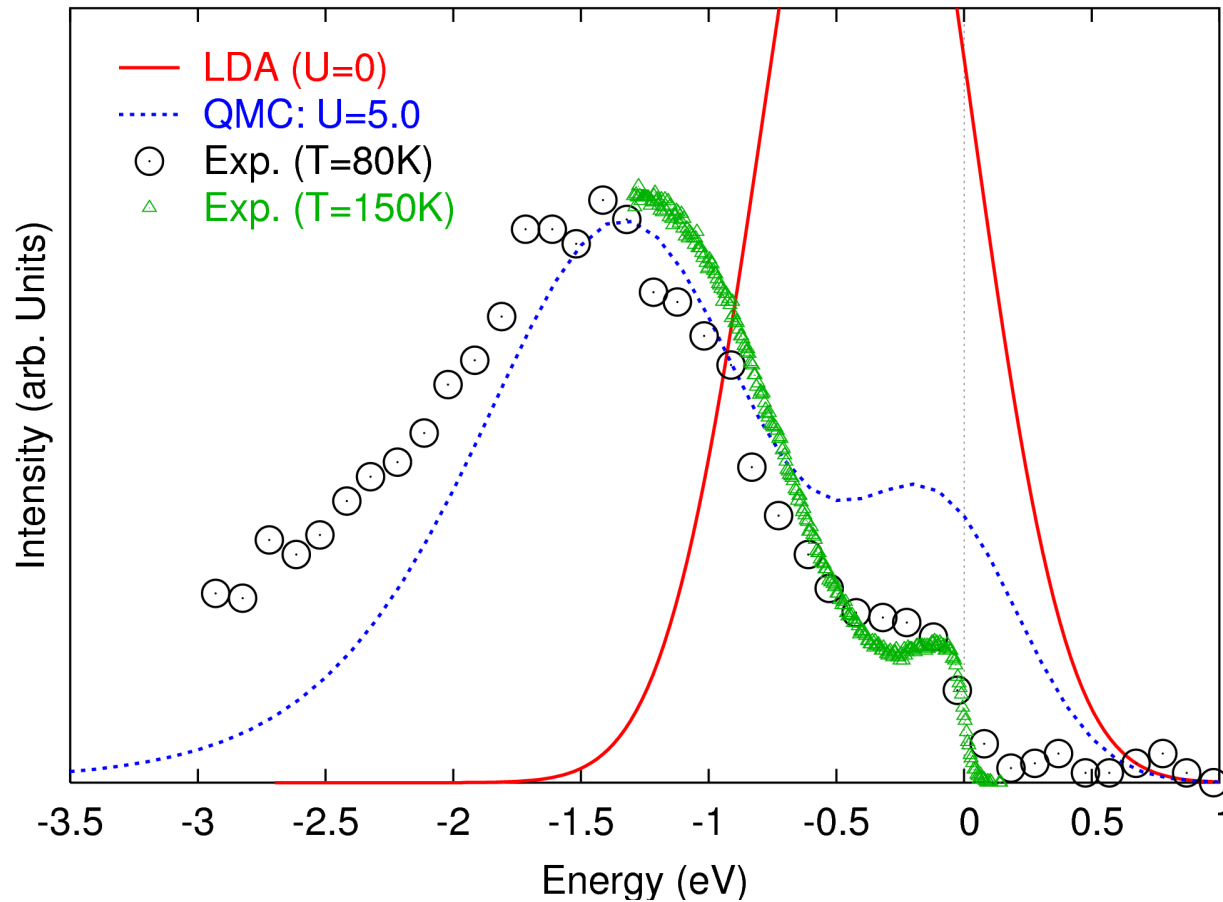
LDA+DMFT(QMC):

Reduction of quasiparticle peak,
appearance of Hubbard bands



Method for solving
DMFT matters!

Photoemission spectra for $\text{La}_{1-x}\text{Sr}_x\text{TiO}_3$



[Nekrasov, Held, NB, Poteryaev, Anisimov, Vollhardt, (2000)]

Reasonable accuracy, drastic improvement over LDA

But: old QMC code not accurate near MIT \rightsquigarrow eliminate $\Delta\tau$ discretization error!

LDA+DMFT for general case: multiple inequivalent bands

Now: LDA density of states not enough, need Hamiltonian in localized basis (e.g.: Wannier functions)

For any (orthogonal) \mathbf{k} space basis:

DFT band structure can be Fourier transformed to real space

↪ single-particle Hamiltonian

$$\hat{H}_{\text{LDA}} = \sum_{ilm,jl'm',\sigma} (\delta_{ilm,jl'm'} \varepsilon_{ilm} \hat{n}_{ilm}^{\sigma} + t_{ilm,jl'm'} \hat{c}_{ilm}^{\sigma\dagger} \hat{c}_{jl'm'}^{\sigma}).$$

Here: i, j indices of unit cells
 l, l' indices of atoms in unit cell
 m, m' orbital indices (ranges depend on l, l')
 σ spin

and orbital occupation $\hat{n}_{ilm}^{\sigma} = \hat{c}_{ilm}^{\sigma\dagger} \hat{c}_{ilm}^{\sigma}$

For LDA+DMFT: choose basis which includes localized orbitals, i.e. 3d states.

Now **add interactions** between the localized electrons ($i = i_d$ and $l = l_d$):

$$\hat{H} = \hat{H}_{\text{LDA}} + \frac{1}{2} \sum_{i=i_d, l=l_d} \sum'_{m\sigma, m'\sigma'} U_{mm'}^{\sigma\sigma'} \hat{n}_{ilm\sigma} \hat{n}_{ilm'\sigma'} + \text{spin-flip terms} - \hat{H}_{\text{LDA}}^U$$

Double counting correction $\hat{H}_{\text{LDA}}^U \rightsquigarrow$ shift in chemical potential (Anisimov, 1991)

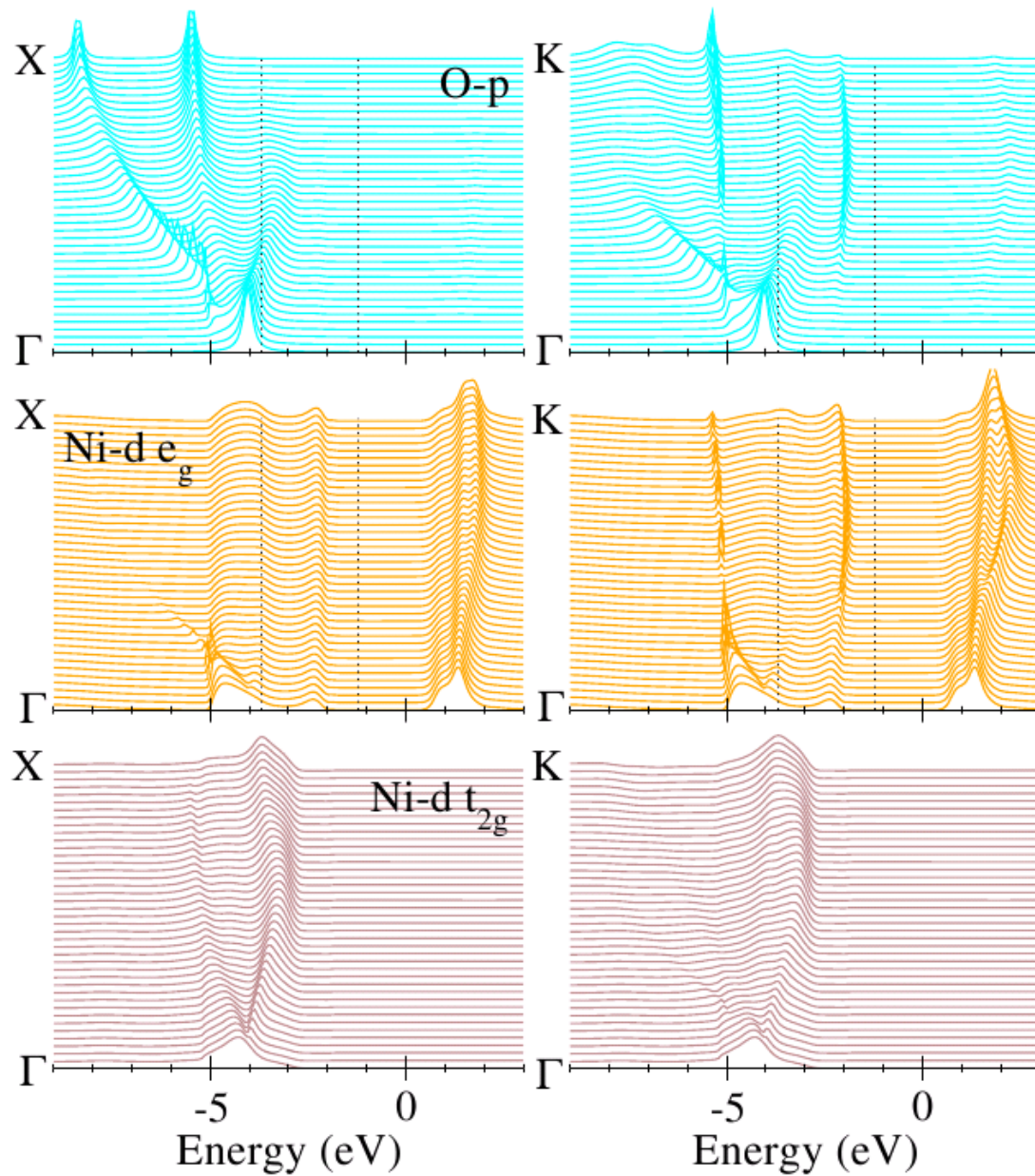
$$\varepsilon_{il_d m}^0 = \varepsilon_{il_d m} - \bar{U}(n_d - \frac{1}{2}) + \frac{J}{2}(n_d - 1) \quad (\text{paramagnetic case})$$

\rightsquigarrow **\mathbf{k} -integrated Dyson equation** (**DMFT self-consistency equation**):

$$\mathbf{G}_{qlm, q'l'm'}(\omega) = \frac{1}{V_B} \int d^3k \left([\omega \mathbf{1} + \mu \mathbf{1} - H_{\text{LDA}}^0(\mathbf{k}) - \Sigma(\omega)]^{-1} \right)_{qlm, q'l'm'}.$$

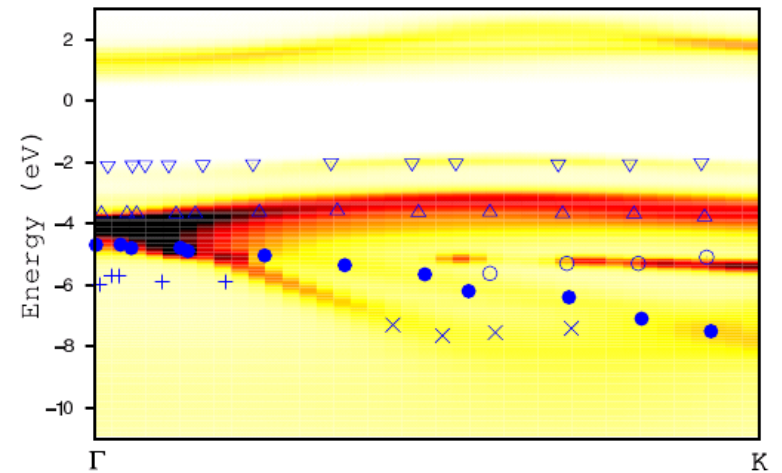
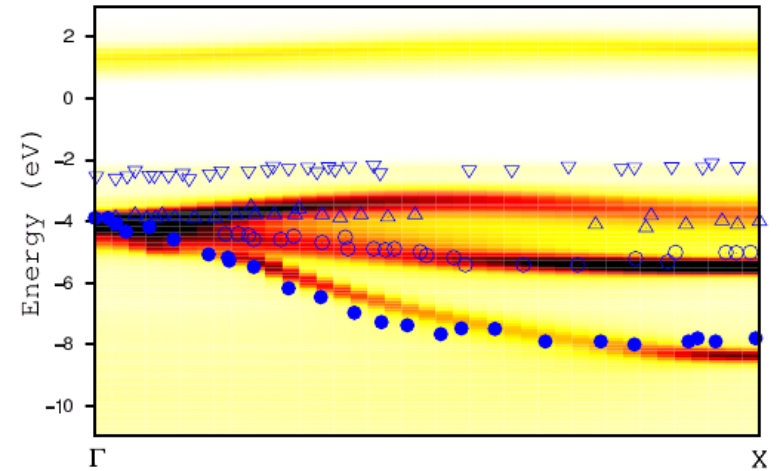
Matrix equation!

Recent example: NiO



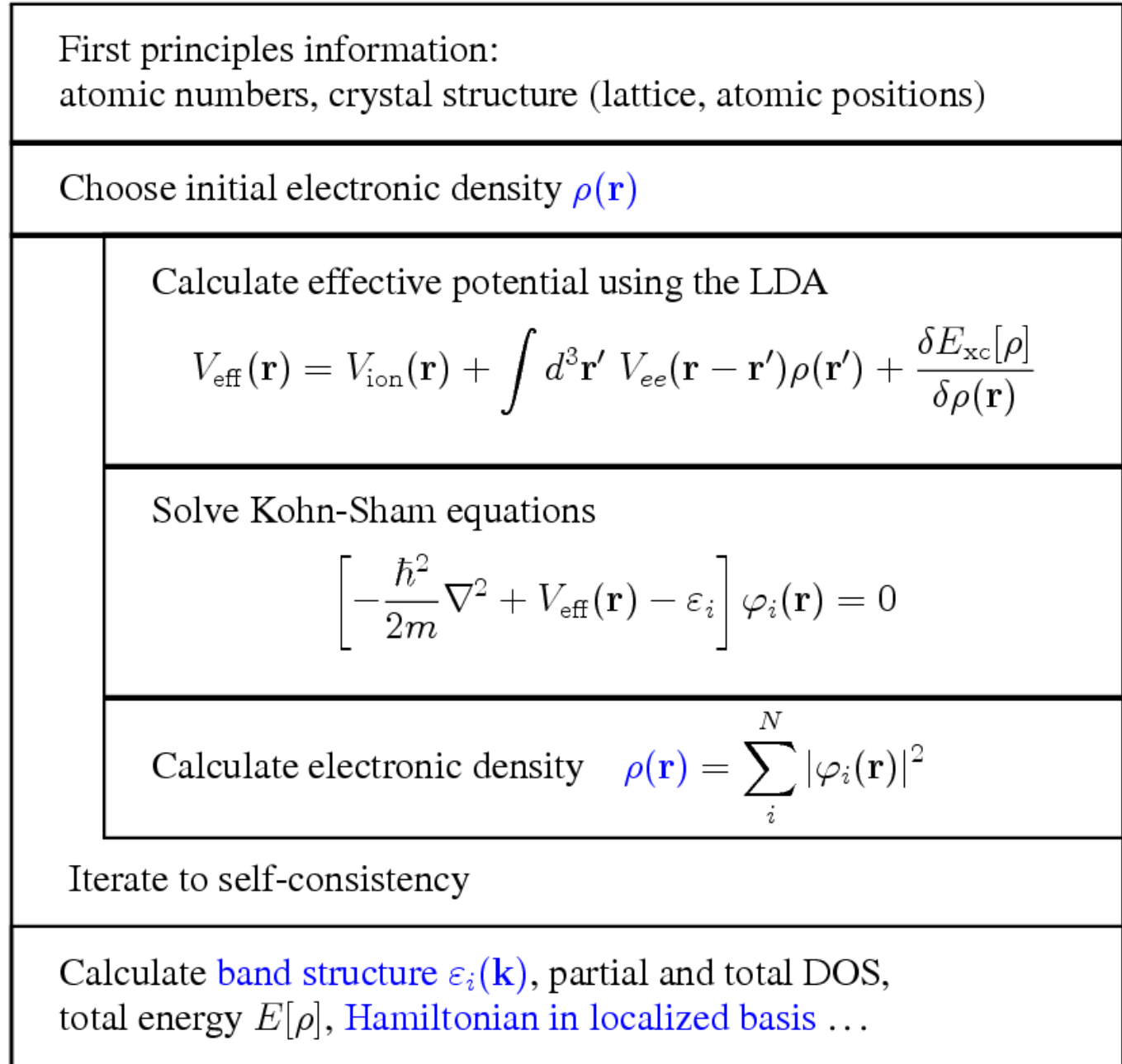
all Ni 3d states + O 2p

$\rightsquigarrow 8 \times 8$ matrices



[Kunes, Anisimov, Skornyakov, Lukoyanov, Vollhardt, arXiv:0705.1692]

Flow diagram for DFT



Flow diagram for DMFT

Choose an initial self-energy Σ

Calculate G from Σ via the k-integrated Dyson equation:

$$G_{qlm,q'l'm'}(\omega) = \frac{1}{V_B} \int d^3k \left([\omega \mathbb{1} + \mu \mathbb{1} - H_{\text{LDA}}^0(\mathbf{k}) - \Sigma(\omega)]^{-1} \right)_{qlm,q'l'm'}$$

$$\mathcal{G}(\omega) = (G^{-1}(\omega) + \Sigma(\omega))^{-1}$$

Calculate G from \mathcal{G} via the DMFT single-site problem

$$G_{\nu m}^{\sigma}(\tau) = -\frac{1}{Z} \int \mathcal{D}[\psi] \mathcal{D}[\psi^*] \psi_m^{\sigma} \psi_m^{\sigma*} e^{\mathcal{A}[\psi, \psi^*, \mathcal{G}^{-1}(\tau)]}$$

$$\Sigma_{\text{new}}(\omega) = \mathcal{G}^{-1}(\omega) - G^{-1}(\omega)$$

Iterate with $\Sigma = \Sigma_{\text{new}}$ until convergence, i.e. $\|\Sigma - \Sigma_{\text{new}}\| < \epsilon$

Problem: occupation of LDA orbitals may have changed \rightsquigarrow charge inconsistency!

Auxiliary-field QMC algorithm [Hirsch, Fye (1986)]

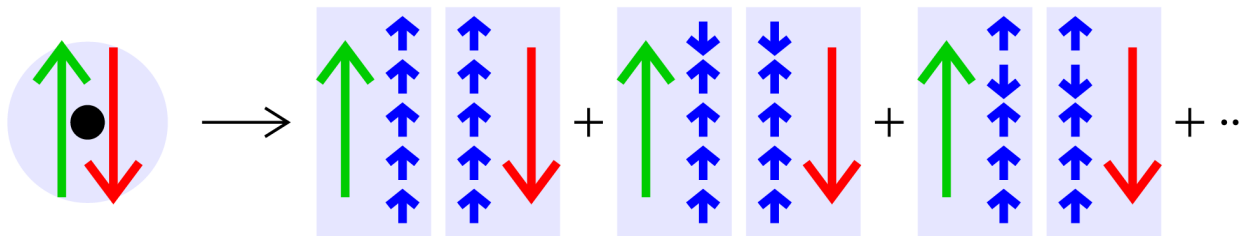
Green-Funktion G in imaginary time (fermionic Grassmann variables ψ, ψ^*):

$$G_{\sigma}(\tau_2 - \tau_1) = \frac{1}{Z} \int \mathcal{D}[\psi] \mathcal{D}[\psi^*] \psi_{\sigma}(\tau_1) \psi_{\sigma}^*(\tau_2) \exp \left[\mathcal{A}_0 - U \sum_{\sigma\sigma'} \int_0^{\beta} d\tau \psi_{\sigma}^* \psi_{\sigma} \psi_{\sigma'}^* \psi_{\sigma'} \right]$$

Discretization $\beta = \Lambda \Delta\tau$, Trotter decoupling $e^{-\beta(\hat{T}+\hat{V})} = \lim_{\Lambda \rightarrow \infty} [e^{-\Delta\tau \hat{T}} e^{-\Delta\tau \hat{V}}]^{\Lambda}$

Use $\hat{n}_{\uparrow} \hat{n}_{\downarrow} = \frac{1}{2} [\hat{n}_{\uparrow} + \hat{n}_{\downarrow} - (\hat{n}_{\uparrow} - \hat{n}_{\downarrow})^2]$; discrete Hubbard-Stratonovich transformation

$$\exp[\Delta\tau U (\hat{n}_{\uparrow} - \hat{n}_{\downarrow})^2 / 2] = \frac{1}{2} \sum_{s=\pm 1} \exp[\lambda s (\hat{n}_{\uparrow} - \hat{n}_{\downarrow})]; \quad \cosh(\lambda) = \exp(\Delta\tau U / 2)$$



Wick theorem:

$$G = \frac{\sum M \det\{M\}}{\sum \det\{M\}}$$

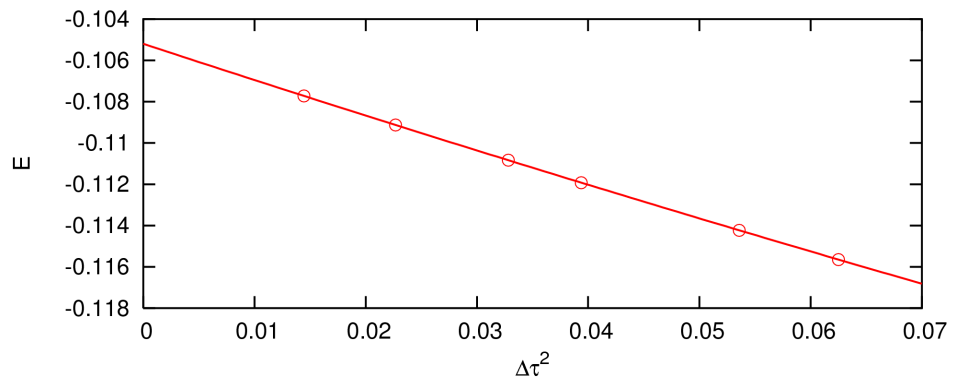
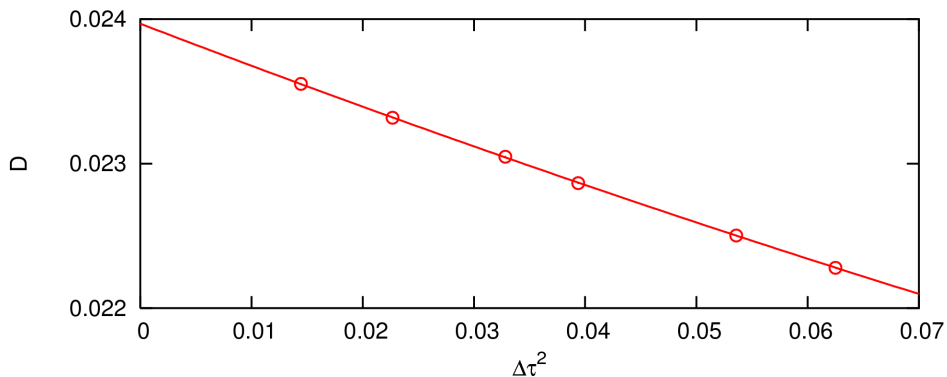
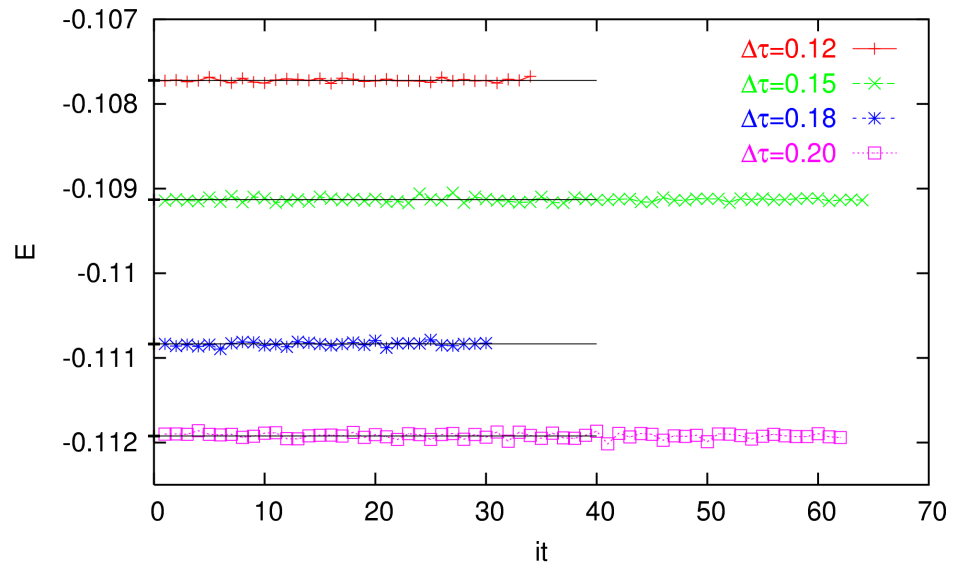
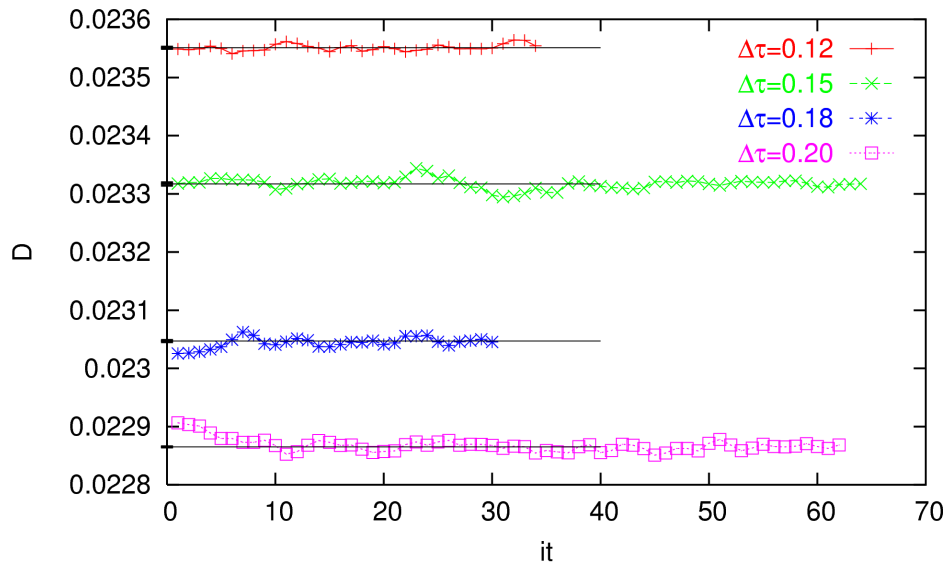
Metropolis MC importance sampling over auxiliary Ising field $\{s\}$: 2^{Λ} configurations

+ numerically exact, + no sign problem, – effort scales as T^{-3}

Contributions to DMFT-QMC error bars:

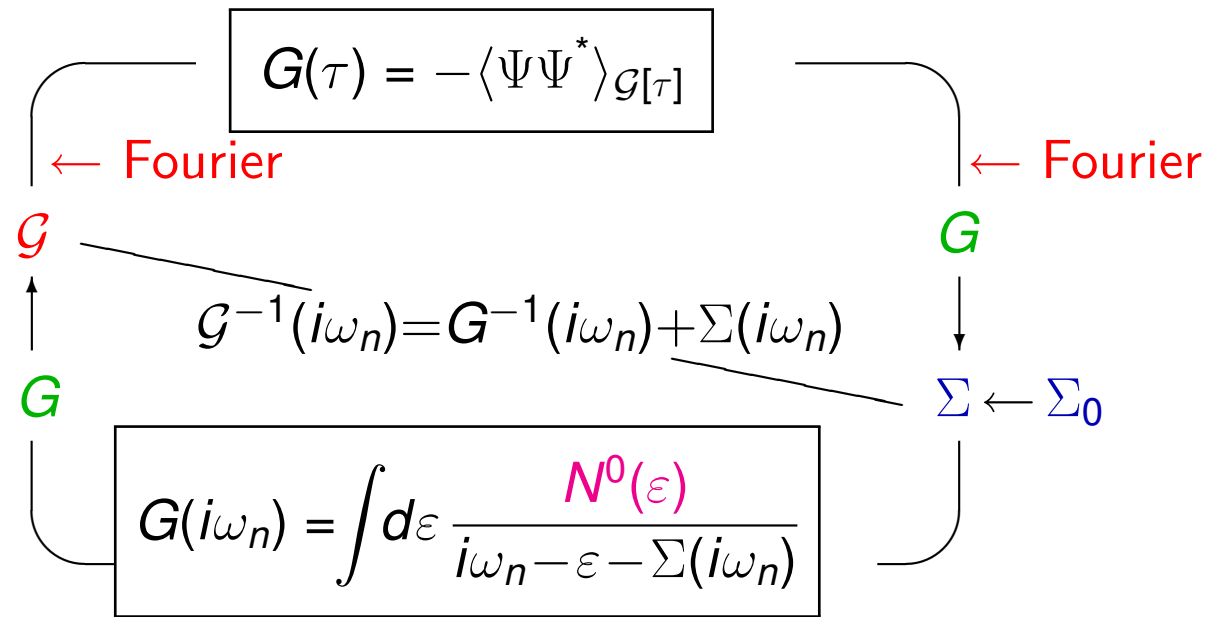
- statistical fluctuations + warm-up
- convergency (of self-consistency cycle)
- discretization (Trotter error and Fourier transform)

Example: half-filled Hubbard model, $U = 5$, $W = 4$, $T = 0.04$ (Mott insulator)

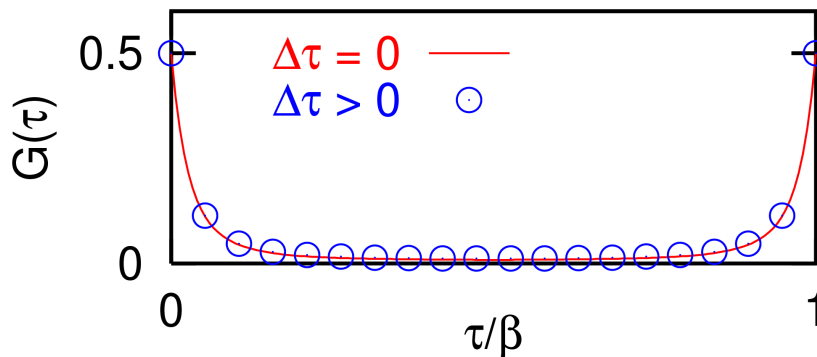


Problems with Fourier transformations in DMFT-QMC cycle

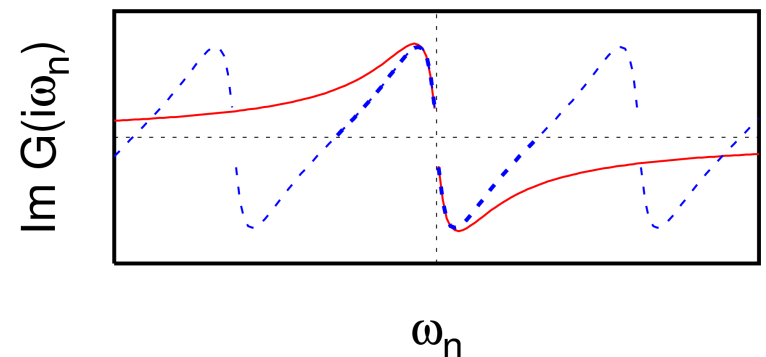
Iterative solution of DMFT equations (for imaginary-time impurity solver)



Naive discrete Fourier transformation \rightsquigarrow oscillations (instead of $G(\omega) \xrightarrow{\omega \rightarrow \infty} 1/\omega$)



naive FT \rightarrow

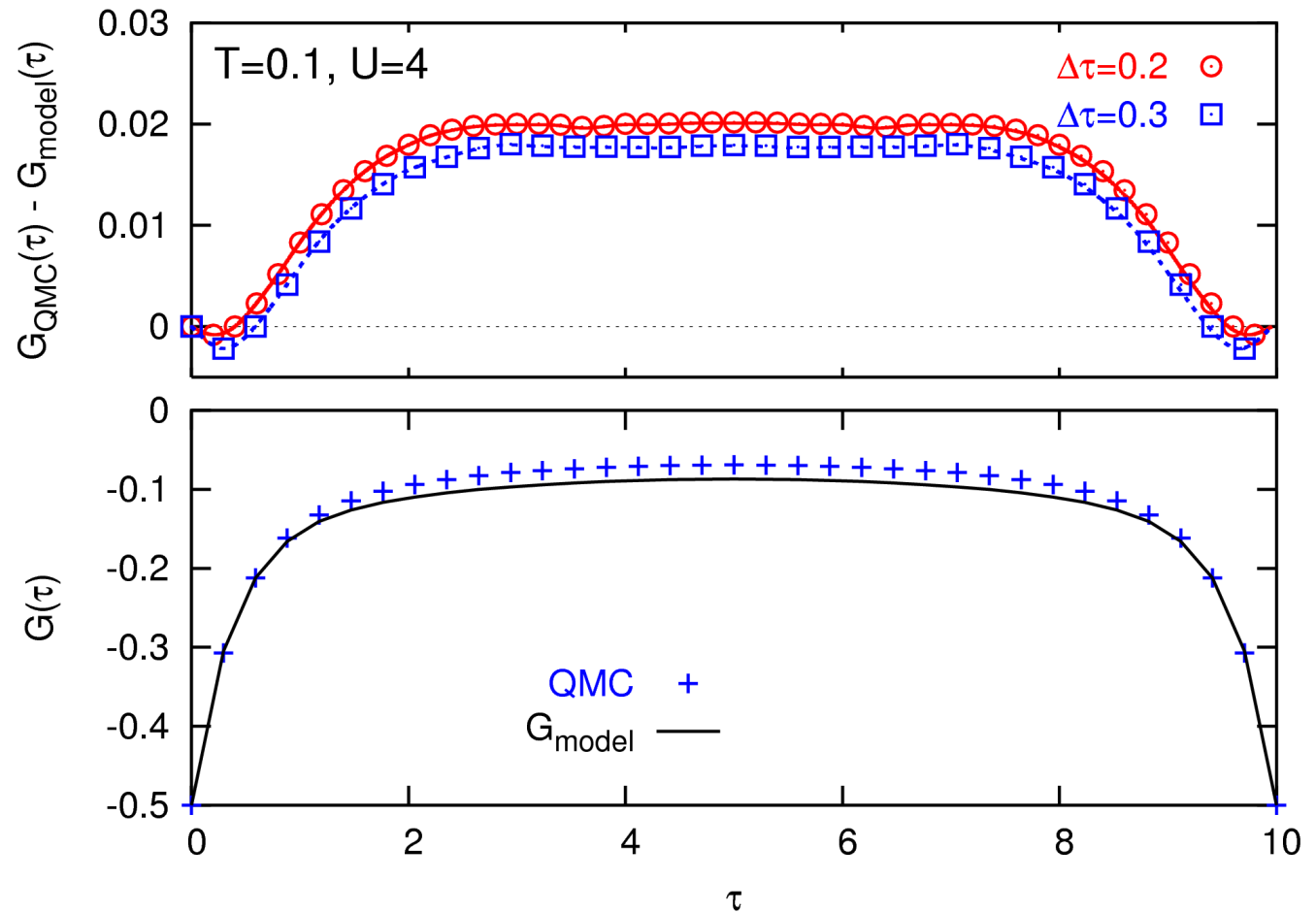


1st solution: correct unphysical behavior for $|\omega| \lesssim \omega_{\text{Nyquist}}$ by transformation [Ulmke]

2nd solution: interpolate $G_{\text{QMC}}(\tau)$ by cubic splines [Jarrell, Krauth, Gull, . . .]

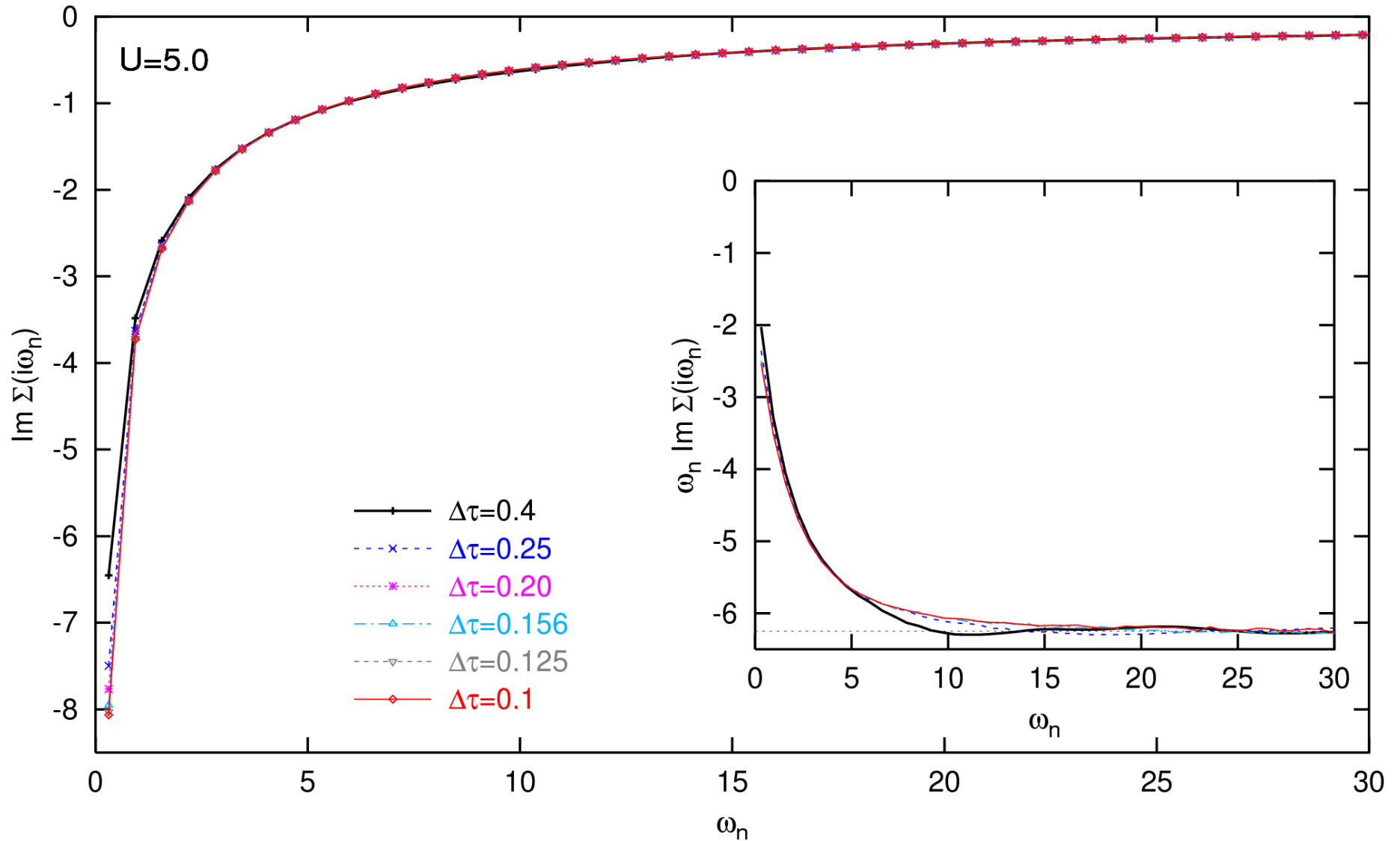
But: $\frac{d^2 G(\tau)}{d\tau^2}$ maximal for $\tau \rightarrow 0, \beta \rightsquigarrow$ natural boundary conditions inappropriate

- adjust boundary cond. [Oudovenko]
- spline-fit only difference w.r.t. reference problem:
 - IPT [Jarrell]
 - high-frequency expansion for $\Sigma(\omega)$ + param. [Knecht, NB]



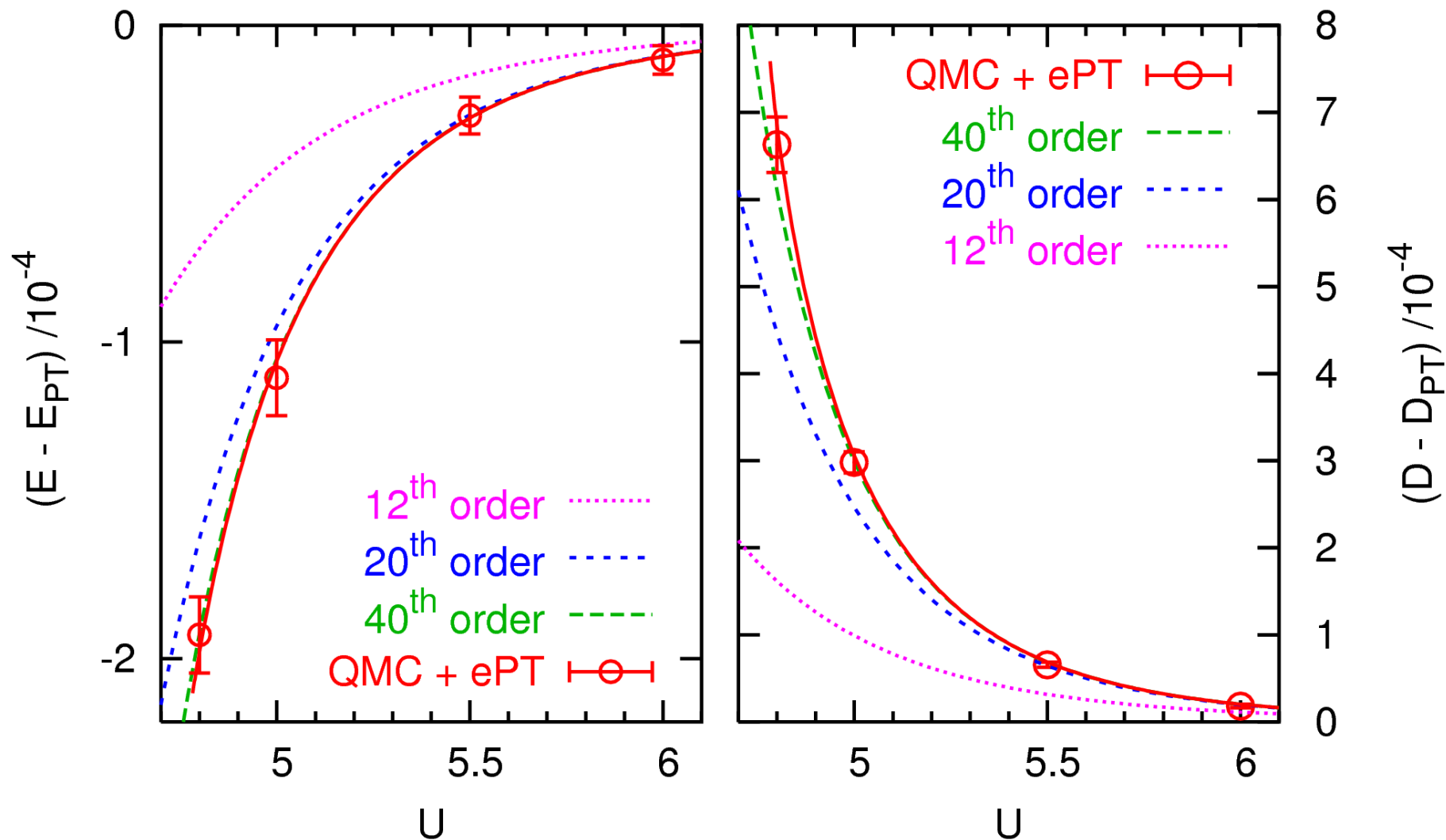
$$\Sigma_{\sigma}(\omega) = U \left(\langle \hat{n}_{-\sigma} \rangle - \frac{1}{2} \right) \omega^0 + U^2 \langle \hat{n}_{-\sigma} \rangle (1 - \langle \hat{n}_{-\sigma} \rangle) \omega^{-1} + \mathcal{O}(\omega^{-2})$$

Sensitive test: self-energy $\Sigma(i\omega_n)$ for insulating phase ($T = 0.1, U = 5.0$)



Rapid convergence at all frequencies for “QMC + $1/\omega$ ” DMFT solver

Extreme QMC precision for Mott insulator



[N. Blümer and E. Kalinowski, Phys. Rev. B 71, 195102 (2005)]

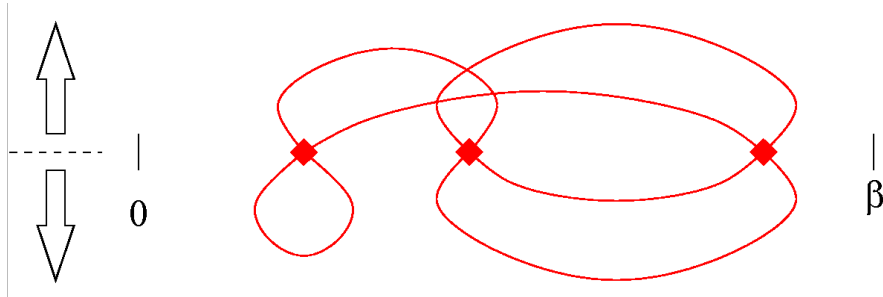
HF-QMC accuracy only challenged by self-energy functional theory (SFT)

QMC DMFT solvers: recent developments

New development: continuous-time QMC algorithms

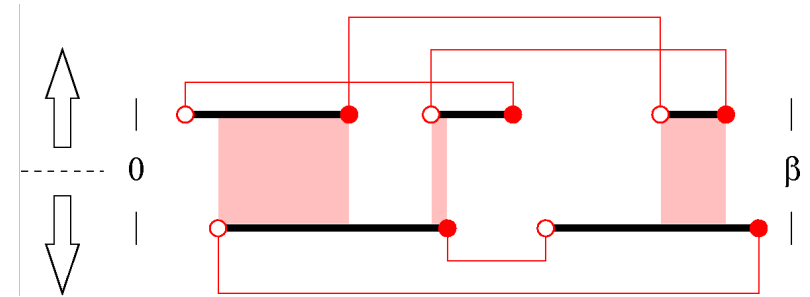
1. weak-coupling expansion

[Rubtsov, Savkin, Lichtenstein, PRB (2005)]



2. hybridization expansion

[Werner et al., PRL (2006)]

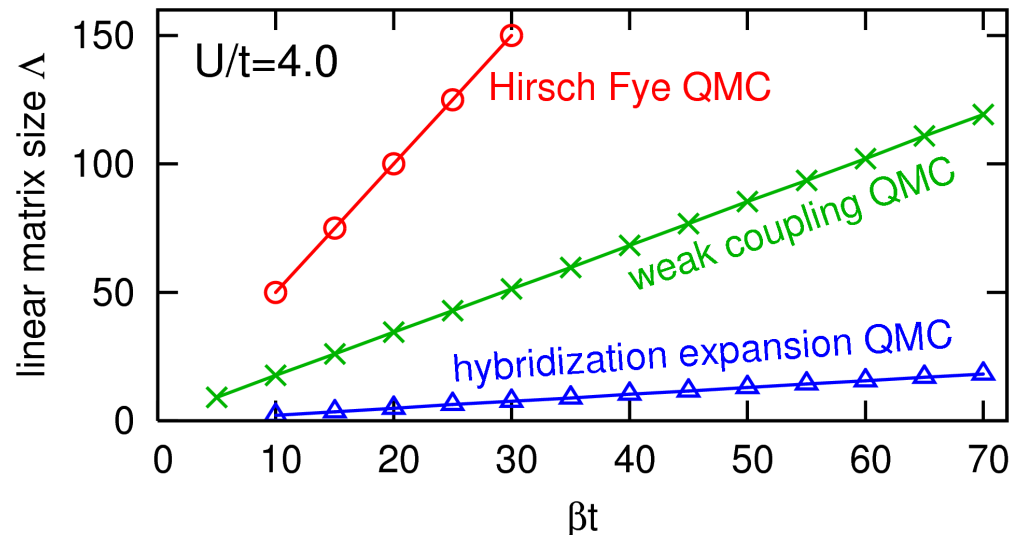


CT-QMC methods: smaller matrices

All QMC methods: effort $\propto \Lambda^3$

Claim [Troyer (2006)]:

CT-QMC more efficient than HF-QMC by orders of magnitude



Performance analysis: CT-QMC methods versus HF-QMC

Performance analysis of continuous-time solvers for quantum impurity models

Emanuel Gull,¹ Philipp Werner,² Andrew Millis,² and Matthias Troyer¹

¹*Institut für theoretische Physik, ETH Zürich, CH-8093 Zürich, Switzerland*

²*Columbia University, 538 West, 120th Street, New York, NY 10027, USA*

Impurity solvers play an essential role in the numerical investigation of strongly correlated electrons systems within the “dynamical mean field” approximation. Recently, a new class of **continuous-time solvers** has been developed, based on a diagrammatic expansion of the partition function in either the interactions or the impurity-bath hybridization. We **investigate the performance** of these two complimentary approaches and **compare them to the well-established Hirsch-Fye method**. The results show that the continuous-time methods, and in particular the version which expands in the hybridization, provide **substantial gains in computational efficiency**.

PACS numbers: 71.10.-w, 71.10.Fd, 71.28.+d, 71.30.+h

[\[cond-mat/0609438\]](#)

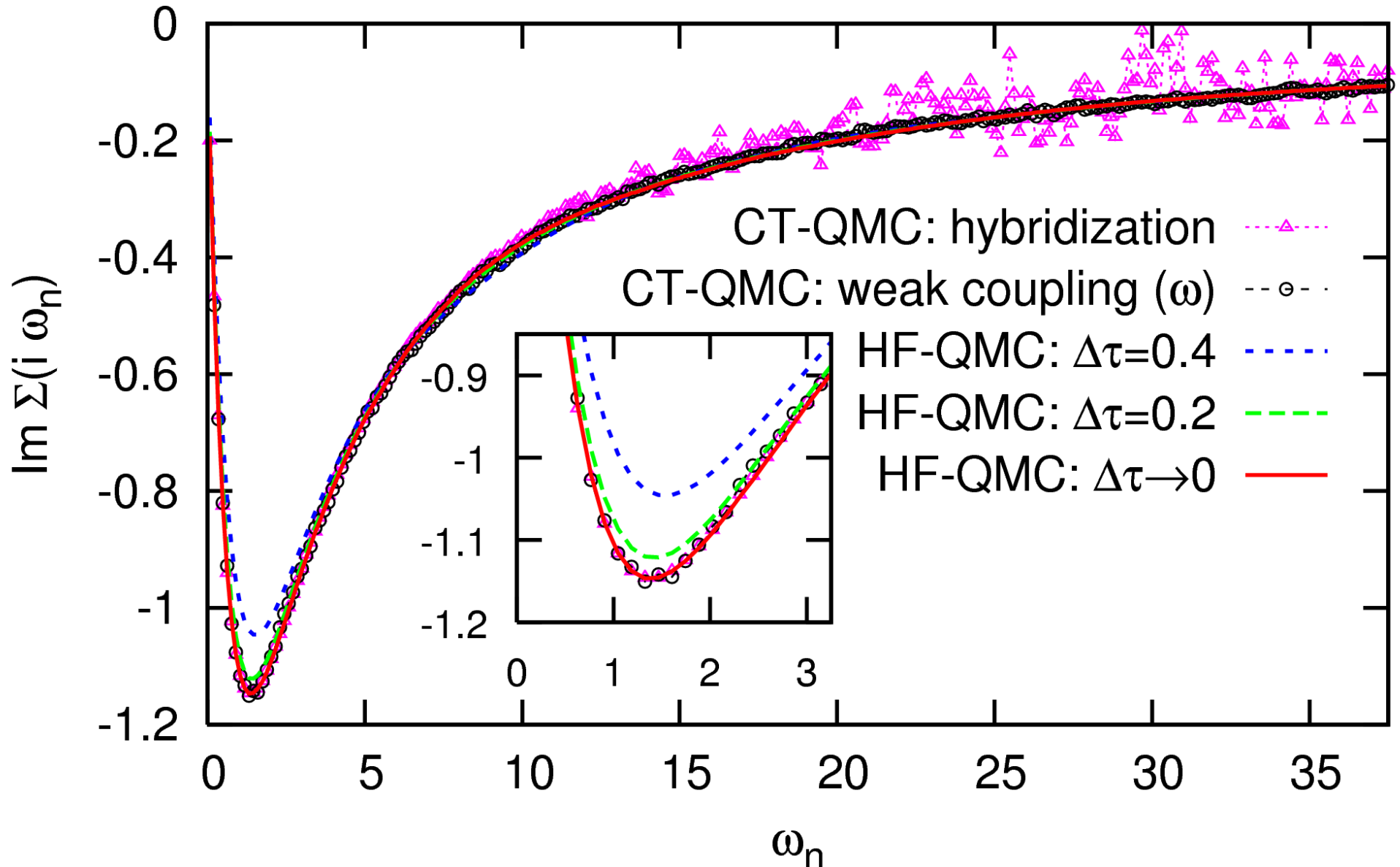
- Test case: 1-band Hubbard model (semi-elliptic DOS, $n = 1$, $W = 4$) for $U = 4$
- Constant computer time: 140 hours on Opteron 244 per data point
- Focus on low temperatures: $T = 1/45$
- Additional results for doped model (also different U)

Good Hirsch-Fye implementation?

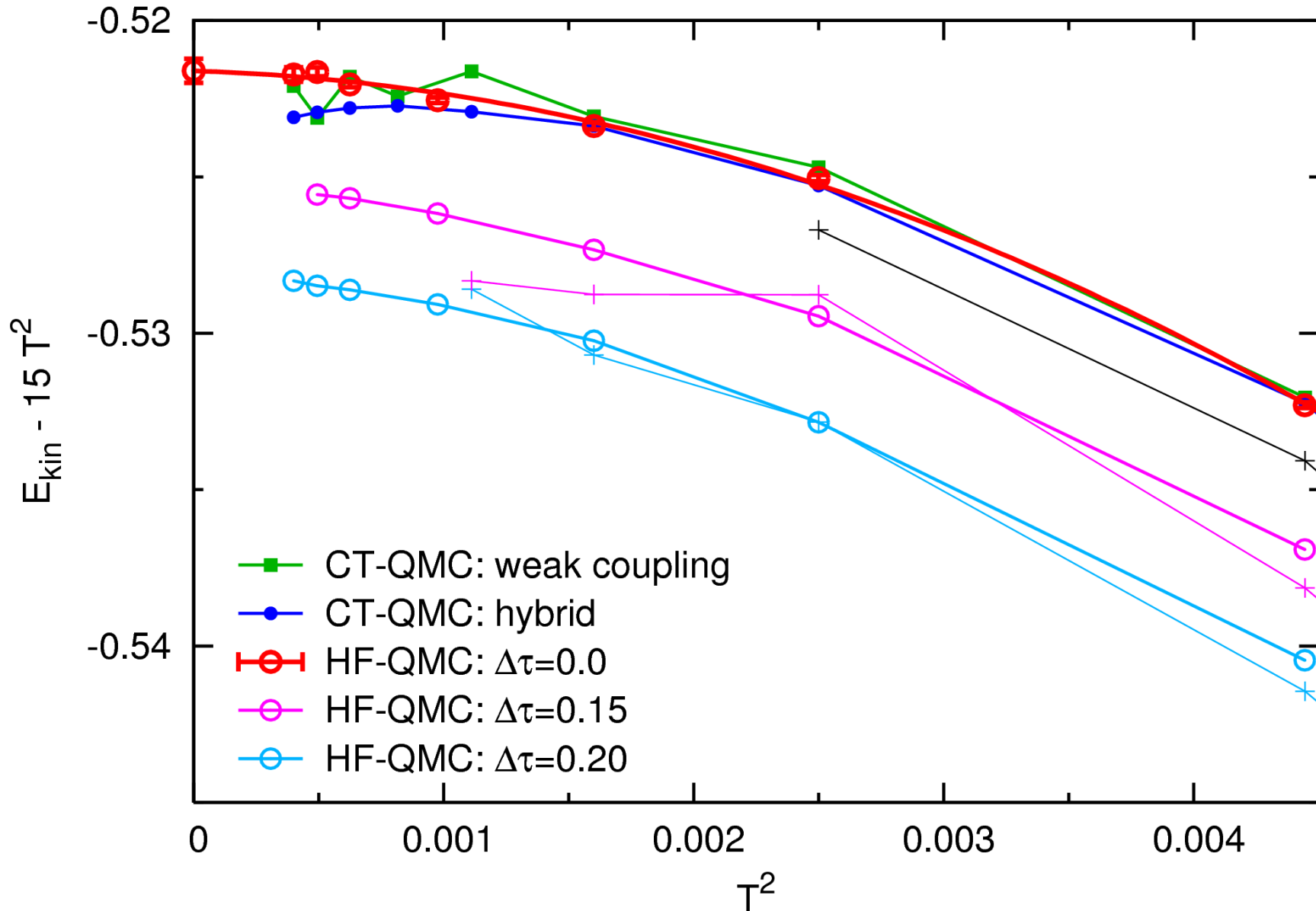
Fair comparison?

Precision of results?

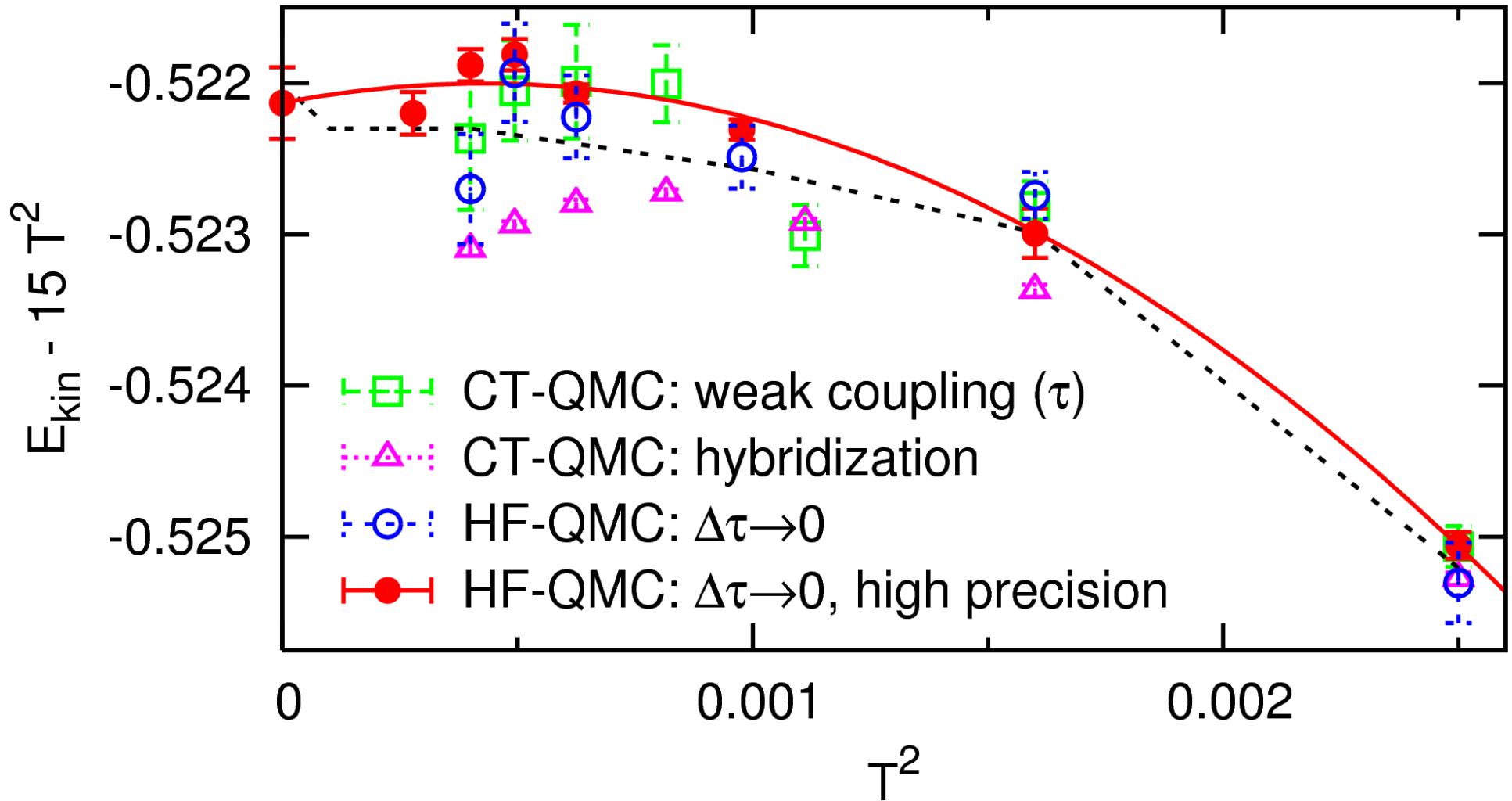
Self-energy on imaginary axis ($T = 1/45$, $U = 4$)



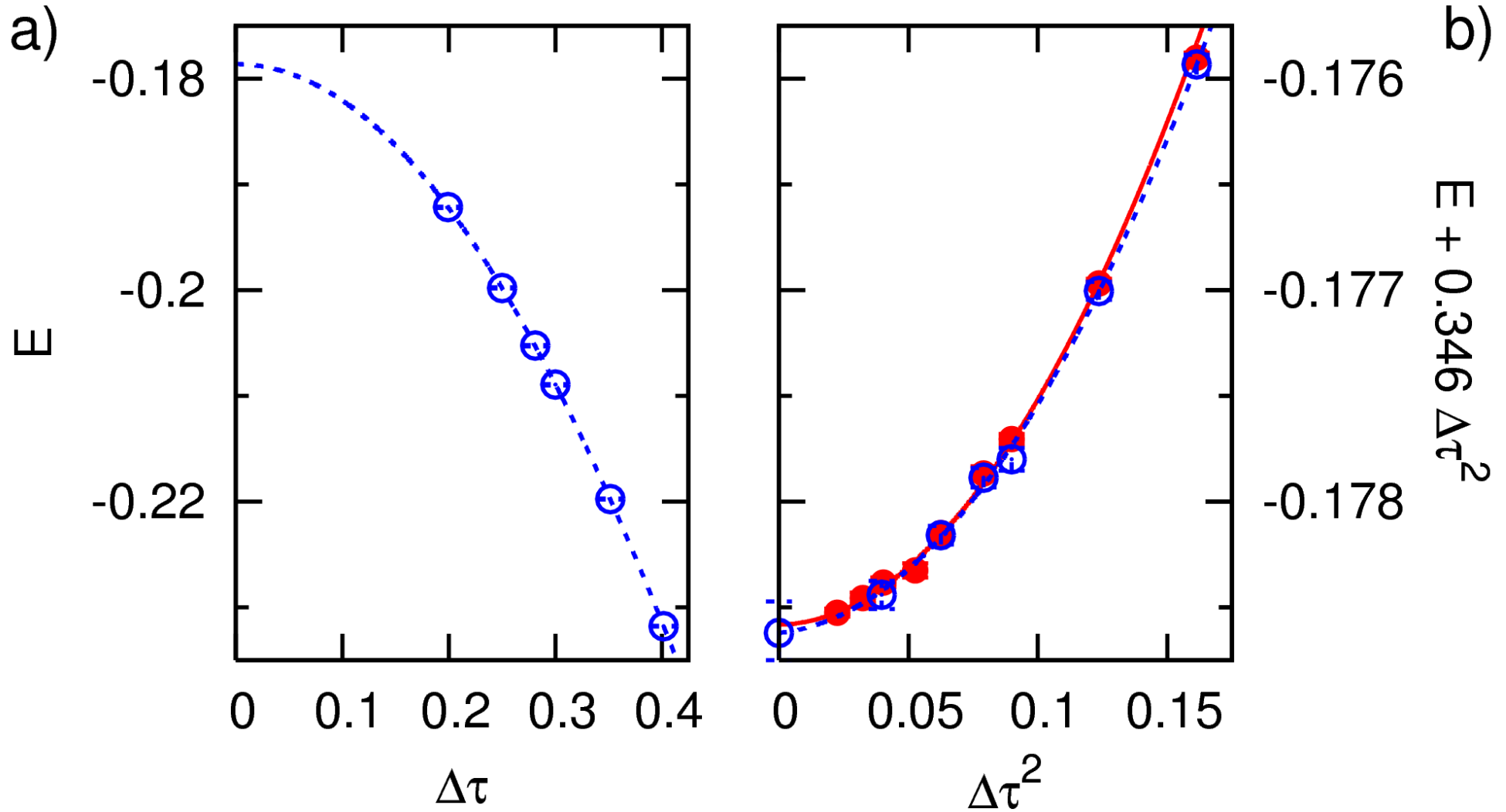
Energetics: kinetic energy for $U = 4$ (first: higher effort for HF-QMC)



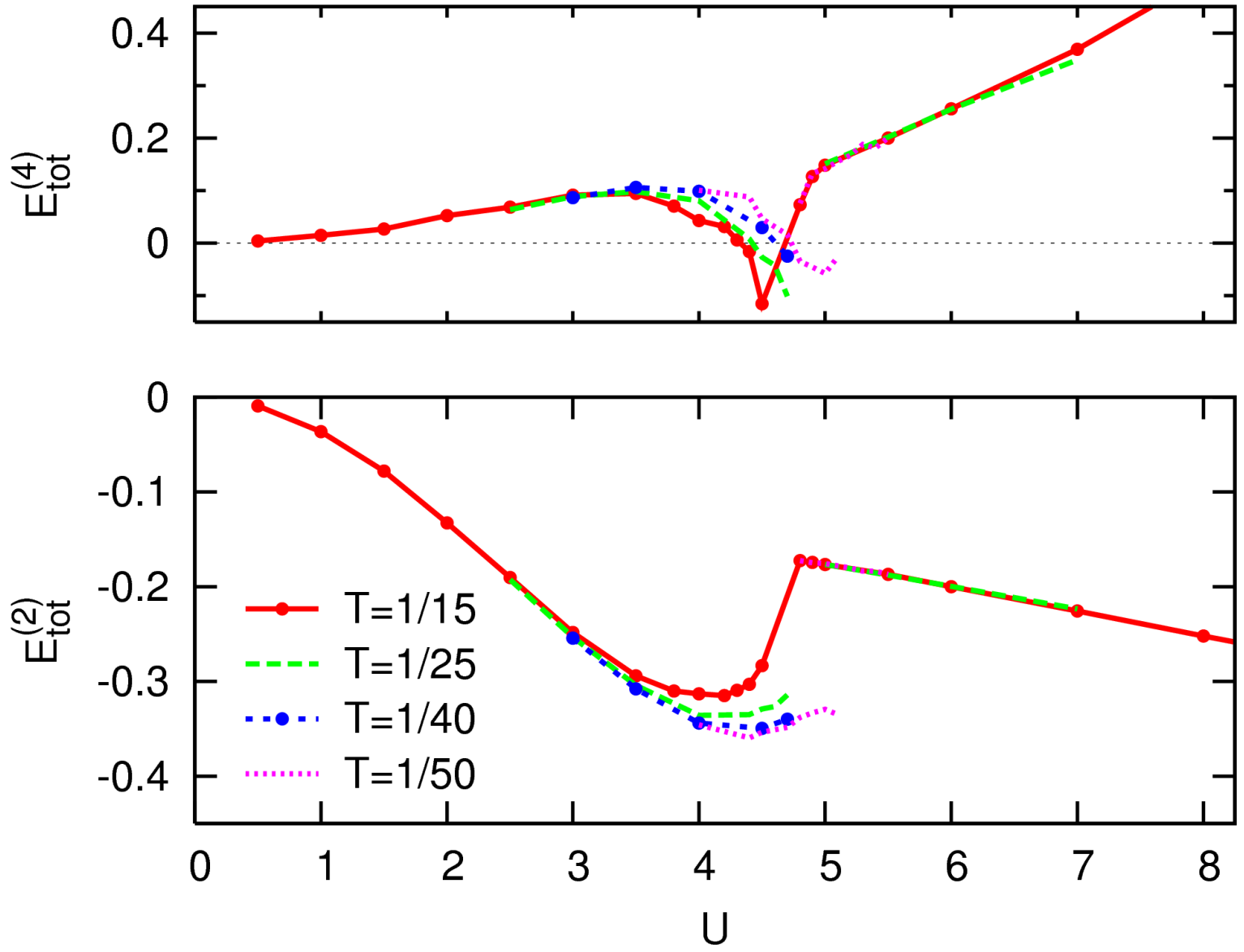
Energetics: kinetic energy for $U = 4$ (same effort for HF-QMC)



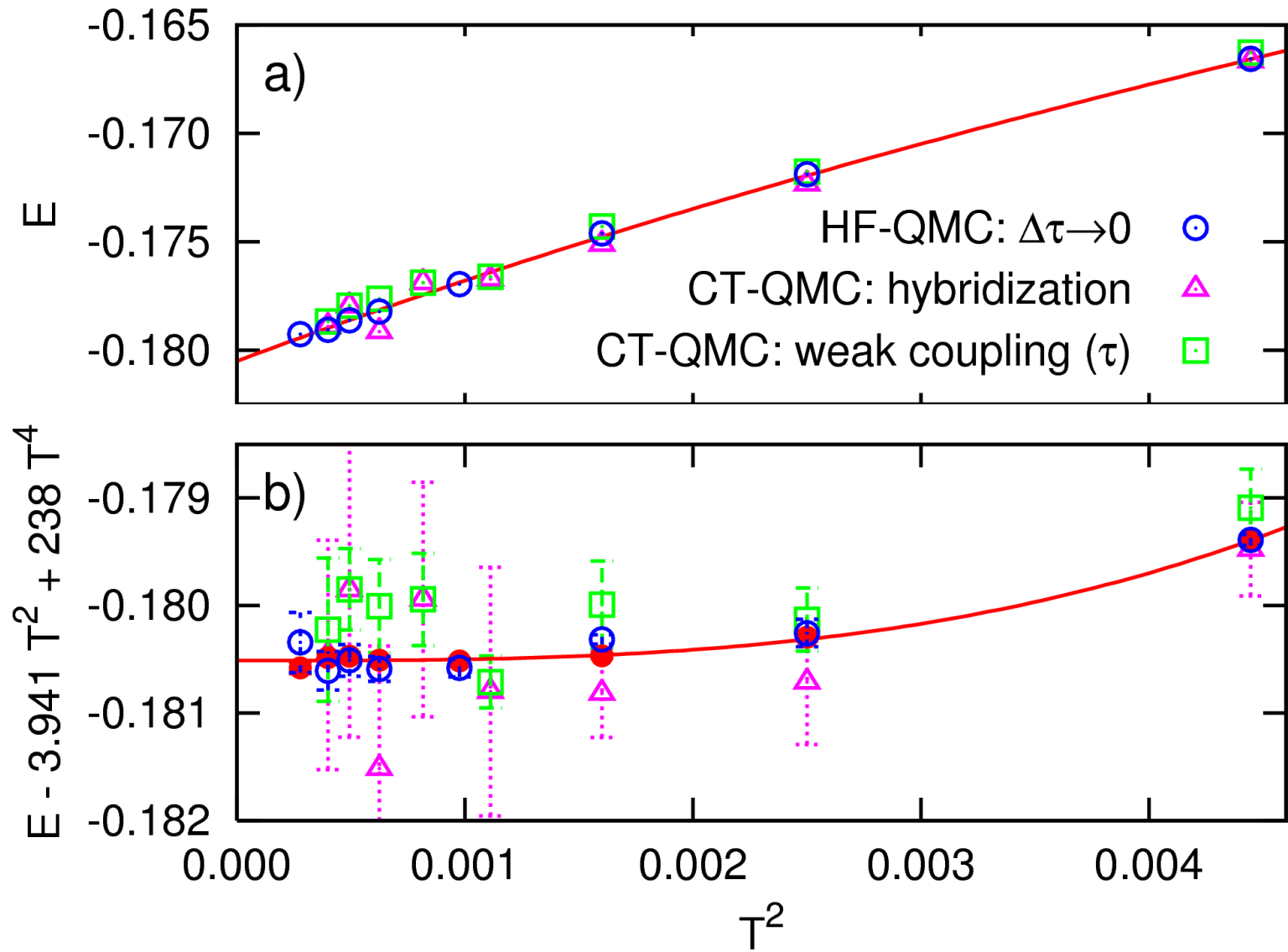
Essential step in HF-QMC: extrapolation $\Delta\tau \rightarrow 0$



$\Delta\tau$ dependence very regular (except at phase transition)

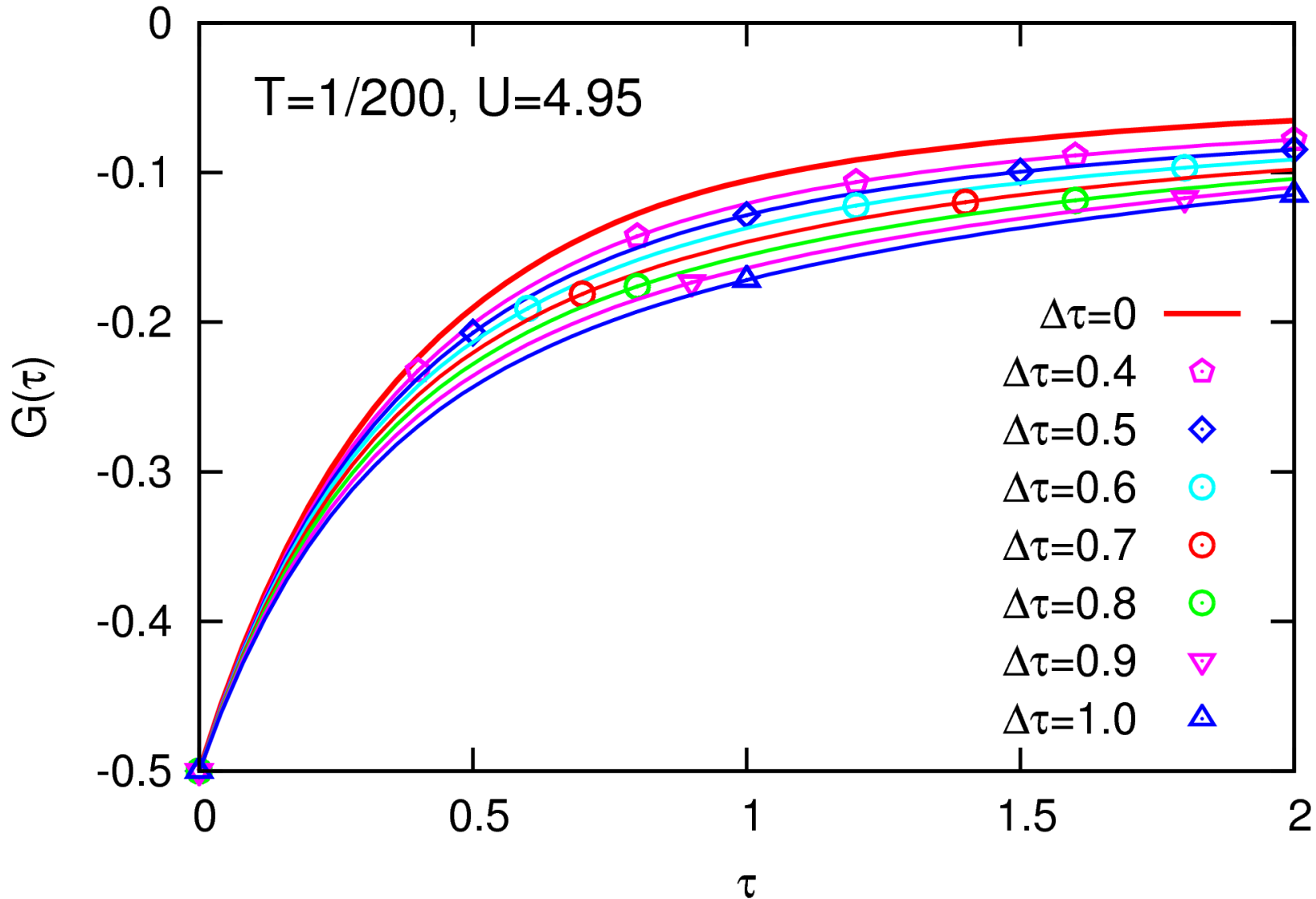


Comparison for total energy



HF-QMC more efficient (much higher precision at same cost) [NB, arXiv:0708.1749]

New: numerically exact Green functions at low T from HF-QMC



Also: first densities of states without discretization error from HF-QMC ...

Summary

Band structures and effects of (strong) electronic correlations

Theory: DFT, (multi-band) Hubbard models, DMFT, LDA+DMFT

High-precision Hirsch-Fye quantum Monte-Carlo algorithm

Efficiency: HF-QMC competitive with continuous-time QMC

Not covered: [Theory of half-metallic double perovskites](#)

Flavor-selective Mott transitions in ultracold quantum gases

Outlook

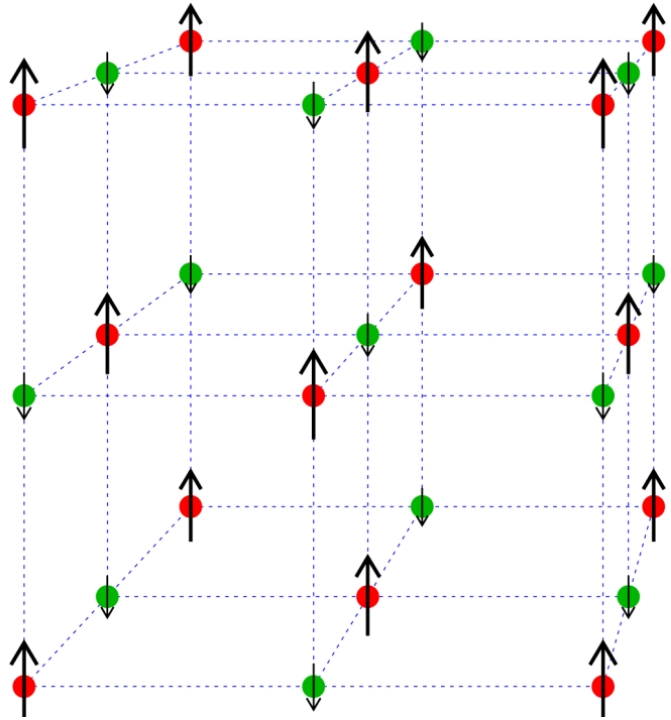
Further improved (better/faster) DMFT solvers

Cluster extensions of DMFT

More complicated systems, full self-consistency, GW+DMFT . . .

Microscopic theory of half-metallic double perovskites

Goal: correlated-electron theory for $\text{Sr}_2\text{FeMoO}_6$ and $\text{Sr}_2\text{FeReO}_6$



Valences ($\text{Sr}_2\text{FeMoO}_6$)

Sr^{2+} [Kr]

Fe^{3+} [Ar] 3d⁵

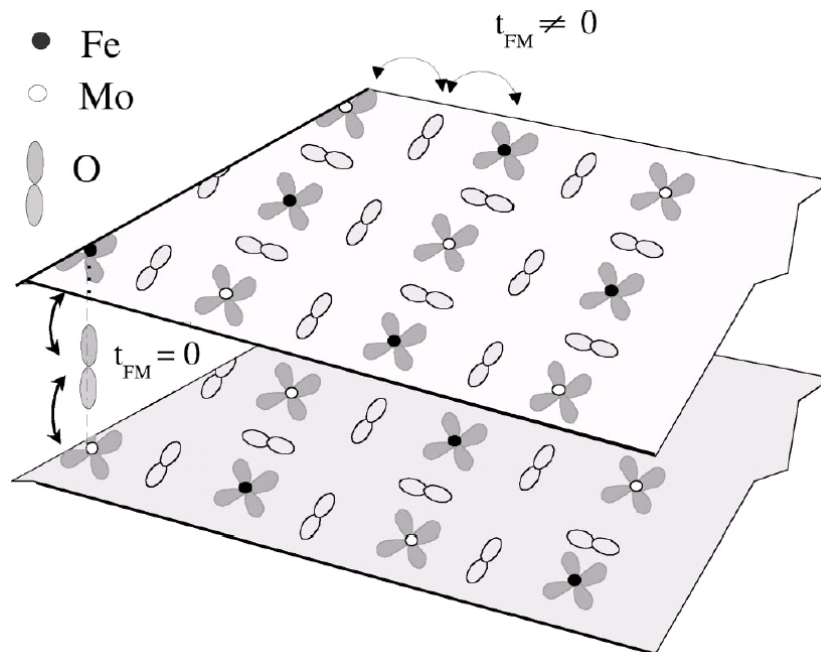
Mo^{5+} [Kr] 4d¹

O^{2-} [Ne]

Cubic symmetry \longrightarrow

3 degenerate t_{2g} bands

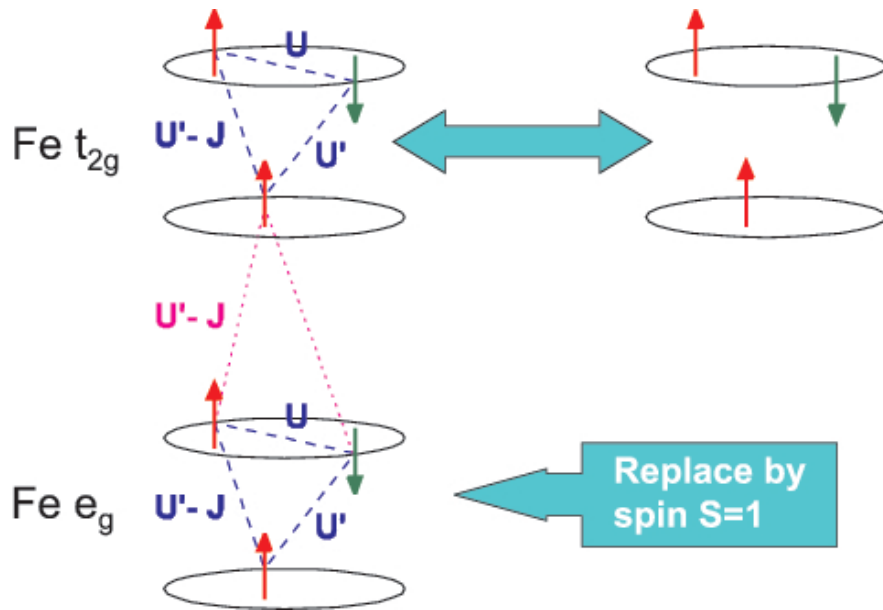
2 degenerate e_g bands



t_{2g} hybridization
Fe - O - Mo/Re

[Petronne, Aligia (2002)]

Microscopic theory of half-metallic double perovskites



Full-Hamiltonian LDA+DMFT calculations for 2-site 3-band Hubbard model with

- Fe t_{2g} - t_{2g} interactions
- Fe t_{2g} - e_g interactions
- Fe - Mo/Re hybridization
- controlled DMFT solver: QMC

$$\begin{aligned}
 H = & \epsilon_F \sum_{i\alpha\sigma} n_{i\alpha\sigma}^f + \epsilon_M \sum_{i\alpha\sigma} n_{i\alpha\sigma}^m \\
 & + U \sum_{i\alpha} n_{i\alpha\uparrow}^f n_{i\alpha\downarrow}^f + \sum_{i\sigma\sigma'} \sum_{\alpha \neq \alpha'} (U' - J \delta_{\sigma\sigma'}) n_{i\alpha\sigma}^f n_{i\alpha'\sigma'}^f - J \sum_{i\alpha} \vec{S}_i \cdot \vec{S}_{i\alpha}^f \\
 & - t_{MF} \sum_{\langle ij \rangle \alpha\sigma} (f_{i\alpha\sigma}^\dagger m_{j\alpha\sigma} + \text{h.c.}) - t_{MM} \sum_{\langle jj' \rangle \alpha\sigma} (m_{j\alpha\sigma}^\dagger m_{j'\alpha\sigma} + \text{h.c.})
 \end{aligned}$$

$$t_{MF} \approx 0.25\text{eV}, \quad t_{MM} \approx 0.15\text{eV}, \quad t_{FF} \approx 0.03\text{eV}, \quad [\text{Phillips et al. (2003)}]$$

Microscopic theory of half-metallic double perovskites

Preliminary DMFT-QMC results (moderate interactions ~ 1 eV)

- t_{2g} fillings
 - $n_{\text{Fe}} = 3.47$
 - $n_{\text{Mo/Re}} = 1.75$
- t_{2g} moments
 - $m_{\text{Fe}} = 1.5\mu_B$
 - $m_{\text{Mo/Re}} = -1.0\mu_B$
- $n = 5.2, m = 2.5\mu_B$

todo:

- ◇ adjust fillings
- ◇ stronger interactions
- ◇ check QMC, MEM ...
- ◇ make contact with experiments

